**Atmospheric
Chemistry
and Physics**
Discussions

Open Access

Biomass burning emissions of trace gases and particles in marine air at Cape Grim, Tasmania, 41° S

S. J. Lawson[1], M. D. Keywood[1], I. E. Galbally[1], J. L. Gras[1], J. M. Cainey[1,2], M. E. Cope[1], P. B. Krummel[1], P. J. Fraser[1], L. P. Steele[1], S. T. Bentley[1,†], C. P. Meyer[1], Z. Ristovski[3], and A. H. Goldstein[4]

[1]Commonwealth Scientific and Industrial Research Organisation, Oceans and Atmosphere Flagship, Aspendale, Australia
[2]formerly from the Bureau of Meteorology, Smithton, Tasmania, Australia
[3]International Laboratory for Air Quality & Health, Queensland University of Technology, Brisbane, Australia
[4]Department of Civil and Environmental Engineering, University of California, Berkeley, USA
[†]deceased

Abstract

Biomass burning (BB) plumes were measured at the Cape Grim Baseline Air Pollution Station during the 2006 Precursors to Particles campaign, when emissions from a fire on nearby Robbins Island impacted the station. Measurements made included non methane organic compounds (NMOCs) (PTR-MS), particle number size distribution, condensation nuclei (CN) > 3 nm, black carbon (BC) concentration, cloud condensation nuclei (CCN) number, ozone (O_3), methane (CH_4), carbon monixide (CO), hydrogen (H_2), carbon dioxide (CO_2), nitrous oxide (N_2O), halocarbons and meteorology.

During the first plume strike event (BB1), a four hour enhancement of CO (max $\sim$ 2100 ppb), BC ($\sim$ 1400 ng m^{-3}) and particles > 3 nm ($\sim$ 13 000 cm^{-3}) with dominant particle mode of 120 nm were observed overnight. Dilution of the plume resulted in a drop in the dominant particle mode to 50 nm, and then growth to 80 nm over 5 h. This was accompanied by an increase in O_3, suggesting that photochemical processing of air and condensation of low volatility oxidation products may be driving particle growth.

The ability of particles > 80 nm (CN80) to act as CCN at 0.5 % supersaturation was investigated. The ΔCCN / ΔCN80 ratio was lowest during the fresh BB plume (56 %), higher during the particle growth event (77 %) and higher still (104 %) in background marine air. Particle size distributions indicate that changes to particle chemical composition, rather than particle size, are driving these changes. Hourly average CCN during both BB events were between 2000–5000 CCN cm^{-3}, which were enhanced above typical background levels by a factor of 6–34, highlighting the dramatic impact BB plumes can have on CCN number in clean marine regions.

During the 29 h of the second plume strike event (BB2) CO, BC and a range of NMOCs including acetonitrile and hydrogen cyanide (HCN) were clearly enhanced and some enhancements in O_3 were observed (ΔO$_3$ / ΔCO 0.001–0.074). A shortlived increase in NMOCs by a factor of 10 corresponded with a large CO enhancement, an increase of the NMOC / CO emission ratio (ER) by a factor of 2–4 and a halving of the BC / CO ratio. Rainfall on Robbins Island was observed by radar during this period

which likely resulted in a lower fire combustion efficiency, and higher emission of compounds associated with smouldering. This highlights the importance of relatively minor meterological events on BB emissions.

Emission factors (EF) were derived for a range of trace gases, some never before reported for Australian conditions, (including hydrogen, phenol and toluene) using a calculated ER to CO and a published CO EF. The EF derived for most species are comparable to other temperate Australian studies but lower than Northern Hemisphere temperate studies.

This work demonstrates the substantial impact that BB plumes have on the composition of marine air, and the significant changes that can occur as the plume is diluted and interacts with other emission sources. We also provide new trace gas and particle EF for temperate southern Australia.

1 Introduction

Biomass burning (BB) is the largest global source of primary carbonaceous fine aerosols and the second largest source of trace gases (Akagi et al., 2011). Species directly emitted from fires include carbon dioxide (CO_2), methane (CH_4), carbon monoxide (CO), nitrogen oxides (NO_x), ammonia (NH_3), non methane organic compounds (NMOCs), carbonyl sulfide (COS), sulfur dioxide (SO_2) and elemental and organic carbonaceous and sulphate-containing particles (Keywood et al., 2011). Secondary species that are formed from BB precursors include ozone (O_3), oxygenated NMOCs and inorganic and organic aerosol (OA). The complex mixture of reactive gases and aerosol that make up BB plumes can act as short lived climate forcers (Keywood et al., 2011). While BB plumes often have the greatest impact on the atmosphere close to the source of the fire, once injected into the free troposphere (FT) plumes may travel long distances, so that climate and air quality affects may be regional or even global. A recent modelling study by Lewis et al. (2013) for example highlighted the large con-

tribution that BB emissions make to the burden of several NMOC in the background atmosphere, particularly in the Southern Hemisphere.

With some studies predicting that future changes to the climate will result in increasing fire frequency (Keywood et al., 2011), it is essential to understand the composition of fresh plumes, how they vary temporally and spatially, and the way in which the chemical composition is transformed with aging. This will provide the process understanding to allow models to more accurately predict regional air quality impacts and long term climate affects of BB.

Characterising BB plumes is challenging for several reasons, and significant knowledge gaps still exist. BB plumes contain extremely complex mixtures of trace gases and aerosols, which vary substantially both spatially and temporally. The initial composition of BB plumes is dependent on the combustion process and efficiency of combustion, which has a complex relationship with environmental variables. Combustion efficiency (CE) is a measure of the fraction of fuel carbon completely oxidised to CO_2. However it is difficult to measure all the carbon species required to calculate CE, and so modified combustion efficiency (MCE), which closely approximates the CE, is often used instead, where $MCE = \Delta CO_2 / (\Delta CO + \Delta CO_2)$ (Ferek et al., 1998) where Δ refers to excess or above-background quantities. The efficiency of fire combustion depends on fuel size, density and spacing, fuel moisture content, local meteorology (including temperature, windspeed and precipitation), and terrain (van Leeuwen and van der Werf, 2011), and MCE can vary substantially spatially and temporally within one fire. The EF of trace gas and aerosol species are in many cases strongly tied to the efficiency of combustion. Species such as CO, organic carbon, and NMOCs tend to be emitted at higher rates in smouldering fires which burn with low MCE (i.e. have a negative relationship with MCE), while other species such as CO_2 and black carbon (BC) are emitted at higher rates in flaming fires with higher MCE (e.g. have a positive relationship with MCE) (Andreae and Merlet, 2001).

Once emitted, the composition of BB plumes can change very rapidly, with destruction of highly reactive species, coagulation of particles, and formation of secondary

species such as O_3, oxygenated NMOCs and secondary organic and inorganic aerosol occuring on a timescale of minutes to hours (Akagi et al., 2012; Vakkari et al., 2014). Particles typically become more oxygenated, and particle size often increases as primary particles are coated either with low-volatility oxidation products of co-emited organic and inorganic gases, or with co-emited semi volatile primary organics (Sahu et al., 2012; Akagi et al., 2012; Vakkari et al., 2014). Changes that occur in the composition of the plume can be highly variable and drivers of variability are difficult to quantify. One example is the large variability in the net OA enhancement in aged BB plumes, with studies reporting both enhancements and decreases in the OA / CO ratio with plume aging (Yokelson et al., 2009; Hennigan et al., 2011; Cubison et al., 2011; Akagi et al., 2012; Hecobian et al., 2012).

While BB is recognised as a major source of CCN (Andreae et al., 2002), the hygroscopicity of fresh BB particles varies enormously from weakly to highly hygroscopic and fuel type appears to be a major driver of the variability (Pratt et al., 2011; Engelhart et al., 2012; Petters et al., 2009) along with particle morphology (Martin et al., 2013). As particles age, in addition to becoming larger, they also generally become more hygroscopic and more easily activated to CCN. However, this is dependent on the initial composition and hygroscopicity of the particle, as well as the hygroscopicity of the coating material (Martin et al., 2013; Engelhart et al., 2012). Most studies of CCN in BB plumes to date have been chamber studies, and there are few ambient studies which have examined the ability of BB particles to act as CCN in fresh and aged plumes.

Ozone is typically destroyed by reaction with nitric oxide (NO) in close proxmity to the fire, however once the plume is diluted, O_3 enhancement is often observed (typically normalised to CO). In a recent summary of a number of studies, the enhancement of O_3 to CO typically increases with the age of the plume (Jaffe and Wigder, 2012). However there is significant variation in O_3 enhancements observed between studies which is thought to be dependent on several factors such as precursor emissions (resulting from fuel and combustion efficiency), meteorology, the aerosol affect on plume chemistry

and radiation, and photochemical reactions. Many challenges remain in modelling the transformation processes that occur in BB plumes, such as O_3 formation and changes to particle properties, in part due to a lack of high-quality real-time observations (Jaffe and Wigder, 2012; Akagi et al., 2012).

In recent years there have been a number of intensive field and laboratory studies which have characterised both fresh emissions and aged BB emissions. However there are several regions of the globe where BB emissions, including emission factors (EF), have been sparsely characterised. For example, EF data has been published for only a few trace gases in the temperate forests of Southern Australian (Volkova et al., 2014; Paton-Walsh et al., 2005, 2008, 2012, 2014). The lack of Australian temperate EF was evident in a recent compilation of EF by Akagi et al. (2011), in which all temperate EF reported were from the Northern Hemisphere (NH) from mostly coniferous forests. Species emitted during combustion can be strongly dependent on vegetation type (e.g. Simpson et al., 2011), and EFs from NH coniferous forests are unlikely to be representative of Australia's temperate dry sclerophyll forests. Using EF from boreal and tropical forest fires to model BB plumes in temperate regions adds uncertainty to the model outcomes (Akagi et al., 2011), and more detailed chemical measurements of BB plumes in the Southern Hemisphere temperate regions are needed.

An increasingly wide range of sophisticated instruments are being used to measure the trace gas and aerosol composition and microphysical properties in BB plumes. This has lead to a higher proportion of NMOC being quantified than ever. Despite this, there is significant evidence that a large proportion of NMOCs in BB plumes are still not being identified. A compilation of NMOC measurements from 71 laboratory fires using a range of techniques, found that the mass of unidentified NMOC was significant (up to 50 %) (Yokelson et al., 2013), though recent work using high-resolution proton transfer reaction – time of flight – mass spectrometry (PTR-TOF-MS) has allowed at least tentative identification of up to 93 % of NMOC (Stockwell et al., 2015). Flow reactor experiments have indicated the mass of OA formed in aged BB plumes exceeds the mass of known NMOC precursors, suggesting either unknown NMOC precursors,

and/or highlighting the important contribution of semi and intermediate volatile species to the increase in OA observed (Ortega et al., 2013). These studies highlight the need to include these unidentified and tentatively identified gas phase organics in models to capture the additional reactivity and contribution to OA they provide.

Finally, with increasing global population and urbanisation, it is likely that BB events will increasingly impact human settlements, either through close proximity of fires or transport of plumes to urban areas. Consequently a greater understanding is needed of the interactions between BB and urban emissions. These interactions are complex and have not been significantly studied to date, although there is evidence that interactions between these two sources may significantly change the resulting processes and products in plume aging. For example Jaffe and Wigder (2012) summarise several studies which show that O_3 enhancement in aged BB plumes is greater when the plumes mix with urban emissions, however the mechanisms for this enhancement remain unclear. Hecobian et al. (2012) found higher concentrations of inorganic aerosol components in aged BB plumes that had mixed with urban emissions compared to BB plumes, which were attributed to higher degree of oxidative processing in the mixed plumes.

In this study we have investigated the chemical composition of both fresh and diluted BB plumes in marine air at the Cape Grim Baseline Air Pollution Station. The BB event occurred unexpectedly during the Precursors to Particles campaign (Cainey et al., 2007), which aimed to investigate new particle formation in clean marine air. Despite the opportunistic nature of this work and lack of targeted BB measurements, a wide variety of trace gas and aerosol species were quantified which provide valuable information on the composition of BB plumes in this sparsely studied region of the world.

Title Page

Abstract | Introduction

Conclusions | References

Tables | Figures

|◄ | ►|

◄ | ►

Back | Close

Full Screen / Esc

Printer-friendly Version

Interactive Discussion

2 Methods

2.1 Cape Grim station location and location of fire

The Cape Grim Baseline Air Pollution Station is located near the north-west tip of the island state of Tasmania, Australia, 40.7° S latitude and 144.7° E longitude (see Fig. 1). The station is situated on a cliff 94 m above mean sea level. When the wind blows from the south west sector (the Roaring Forties) the air that impacts the station is defined as Baseline and typically has back trajectories over the Southern Ocean of several days. In northerly wind directions, urban air from the city of Melbourne some 300 km away is transported across the ocean (Bass Strait) to the station. North west Tasmania has a mild temperate climate, with average February temperatues of 15 °C ± 2, RH 75 % ± 12, WS of 9 m s^{-1} ± 4 and 25 mm precipitation.

From 30 January to 24 February 2006 (the Austral late summer), the Precursors to Particles (P2P) campaign was undertaken (Cainey et al., 2007). On the 15 February 2006, in the middle of P2P, a fire was ignited on nearby Robbins Island, which lies across farmland 20 km east of Cape Grim. Robbins Island (9748 ha) is separated from the Tasmanian mainland by a tidal passage 2 km across, and has been a freehold property used for the grazing of sheep and cattle since the 1830s (Buckby, 1988). The vegetation consists of grazed pastures and native vegetation, mostly disturbed coastal heathland (largely endemic *Epacridaceae*, *Leptospermum*) and woodland (*Leptospermum*, *Melaleuca* and *Eucalyptus nitida)* with shrubs interspersed by tussock grasses (Poa spp) and sedges (Kitchener and Harris, 2013). The fire burned 2000 ha, mostly coastal heath, over a period of 2 weeks. On two occasions an easterly wind advected the BB plume directly to the Cape Grim Station. The first plume strike (BB1) occured from 02:00–06:00 (Australian Eastern Standard Time – AEST) on the 16 February, with light easterly winds of 3 m s^{-1} and temperature of 13 °C and RH of 96 %. The second, more prolonged plume strike (BB2) occured from 23:00 AEST on 23 February to 05:00 AEST on the 25 February, with strong easterly winds ranging from 10–16 m s^{-1}, temperatures of 16–22 °C and RH from 75–95 %.

2.2 Measurements

During P2P, a number of additional instruments were deployed to run alongside the routine measurements. All the measurements made during BB1 and BB2 (routine and P2P measurements) are listed in Table 1, with references supplied for further information. Some additional information is provided here. All levels of trace gases are expressed as molar mixing ratios. As the focus of P2P was clean marine air, $PM_{2.5}$ and PM_{10} filter samples were not collected during the BB events.

NMOCs (PTR-MS)

Details on PTR-MS measurements are given in Galbally et al. (2007a) and some additional information is provided here.

The PTR-MS ran with inlet and drift tube temperature of 75 °C, 600 V drift tube, 2.2 mbar drift tube pressure, which equates to an energy field of 140 Td. The O_2^+ signal was ∼ 2 % of the primary ion H_3O^+ signal. The PTR-MS ran in multiple ion detection (MID) mode in which 26 masses were selected. Masses included in this work were identified by reviewing instrument intercomparison studies of BB plumes (Christian et al., 2004; Karl et al., 2007b; de Gouw and Warneke, 2007; Stockwell et al., 2015). Protonated masses were identified as m/z 28 hydrogen cyanide (HCN), m/z 31 formaldehyde (HCHO), m/z 33 methanol (CH_3OH), m/z 42 acetonitrile (C_2H_3CN), m/z 45 acetadehyde (C_2H_4O), m/z 47 formic acid (HCOOH), m/z 59 acetone and propanal (C_3H_6O), m/z 61 acetic acid (CH_3COOH), m/z 63 dimethyl sulphide – DMS (C_2H_6S), m/z 69 furan/isoprene (C_4H_4O/C_5H_8), m/z 71 methacrolein/methyl vinyl ketone – MVK (C_4H_6O), m/z 73 methylglyoxal ($C_3H_4O_2$)/methyl ethyl ketone – MEK (C_4H_8O), m/z 79 benzene (C_6H_6), m/z 93 toluene (C_7H_8), m/z 95 phenol (C_6H_6O), m/z 107 ethylbenzene + xylenes (C_8H_{10}), m/z 121 C_3 benzenes (C_9H_{12}), m/z 137 monoterpenes ($C_{10}H_{16}$). These are expected to be the dominant compounds contributing to these masses. However, due to the inability of the PTR-MS to differentiate between species with the same molecular mass, a contribution from other compounds

not listed here cannot be ruled out. Protonated masses m/z 46, m/z 85, m/z 87, m/z 101, m/z 113 and m/z 153 were measured but not identified, but have been included here with the aim of quantifying as much emitted volatile carbon as possible.

During the campign the PTR-MS was calibrated for the following compounds using certified gas standards from Scott Specialty Gases, USA and National Physical Laboratory, UK: methanol, acetaldehyde, acetone, isoprene, MVK and methacrolein, MEK, benzene, toluene, ethylbenzene, 1,2,4 trimethylbenzene and formaldehyde. Calibration data were used to construct sensitivity plots which were used to calculate approximate response factors for other masses not specifically calibrated. Due to having proton affinities similar to water, formaldehyde and HCN responses are highly dependent on humidity of the sample air. The changing response of the PTR-MS for these compounds was calculated every 10 min by taking the response of the dry formaldehyde calibration gas, then adjusting this based on the measured water content of the sample air and relationship between response and humidity as reported in Inomata et al. (2008). Corrections were made to the response of m/z 61 and m/z 137 for known losses due to fragmentation of acetic acid and monoterpenes at those masses. Dunne et al. (2012) reported a significant interference to the acetonitrile signal at m/z 42 from the ^{13}C isotopologues of $C_3H_5^+$ and the product ion $C_3H_6^+$ from reactions involving O_2^+ and alkanes/alkenes. A detailed correction for this interference was not possible here, due to an absence of m/z 41, and alkane and alkene measurements. However, during a BB event, Dunne et al. (2012) calculated a 20 % contribution to m/z 42 from non-acetonitrile ions: to reflect this interference the m/z 42 signal during the BB events has been reduced by 20 %. Minimum detectable limits (MDLs) were calculated according to the principles of ISO 6869 (ISO, 1995) and ranged from 2–563 ppt for a one hour measurement. Where measured levels were below the MDL, a half MDL value was substituted.

3 Results and discussion

A time series of CO, BC and particle number $> 3\,\text{nm}$ clearly shows the two events (BB1 and BB2) where plumes from the Robbins Island fire impacted the Cape Grim Station (Fig. 2). A detailed times series of these two events are presented here, with discussion of the influence of photochemistry, meteorology and air mass back trajectory on changing composition of trace gases and aerosol.

3.1 Biomass burning event 1 (BB1) 16 February 2006

3.1.1 Brief plume strike, particle growth and ozone enhancement

Figure 3 shows a time series plot from BB1, including both the fresh plume and the changing composition with changing wind direction. A particle size and number contour plot, wind direction, O_3, CO, BC and urban tracer HFC-134a are shown. Periods of interest are labelled as periods A–F (Fig. 3) which are discussed below and summarised in Table 2. Average particle size distributions for periods corresponding to periods A–F are presented in Fig. 4. NMOC data is not available from BB1. The matching air mass back trajectories for periods corresponding to periods A–F are shown in Fig. S1a–f.

Period A. The fresh BB plume is visible from $\sim 02{:}00\text{–}06{:}00$ AEST (Fig. 3) through high particle number concentrations corresponding with elevated CO and BC. The BB particles have a single, broad size distribution with a dominant mode of 120 nm (Fig. 4a), indicating fresh BB aerosol (Janhäll et al., 2010). The O_3 mixing ratio during this period is 10 ppb which is lower than background concentration of about ~ 15 ppb, likely due to titration by NO emitted from the fire. The HYSPLIT back trajectory (Fig. S1a) indicates that air which brought the plume to Cape Grim had previously passed over the north west corner of Tasmania and the Southern Ocean.

Period B. Just after 06:00 AEST (Fig. 3), a wind direction change results in dramatically reduced particle concentration, CO and BC, indicating the BB plume is no longer directly impacting the station. With the sudden reduction in BB tracers, the dominant

mode of the particles drops from about 120 to 50 nm, but the distribution remains broad and uni-modal (Fig. 4a). At around 07:00 AEST, O_3 increases, accompanied by a gradual increase in the dominant mode of particles, indicating a particle growth event. The mean diameter of the particles increases from 50 to 80 nm over a period of 5 h (corresponding to a growth rate of $\sim$ 6 nm h^{-1}), with an O_3 increase from 12 to 20 ppb. This daytime increase in O_3 alongside particle growth is suggestive of photochemical processing of the air, and an increase in particle size due to condensation of low volatility oxidation products. The emission source/s driving this particle growth event are not clear. The BC is elevated above background concentrations between 12–194 ng m^{-3}, vs. 2 ng m^{-3} in background air, suggesting the BB plume is diluted to between 1–14 % during particle growth. CO is elevated only 10 ppb above background during this period. However, unlike the integrated BC measurements, CO is an instanteous measurement every 40 min (Table 1) and it is likely these CO observations have not captured the BB plume influence during this period of high variability (e.g. during mixing of air masses). The HYSPLIT trajectory (Fig. S1b) shows that air arriving at the station during the particle growth event is almost entirely of marine origin but had some contact with the vegetated and sparsely populated North West coast of Tasmania and passes close to the Robbins Island fire before arriving at Cape Grim.

Period C. At midday, the dominant particle mode stops increasing and is stable, and BC drops to background levels, indicating that fire emissions are no longer impacting the station. An easterly wind overnight brings air from the sparsely populated and forrested coast of south eastern Australia (Fig. S1c) which leads to a further decrease in particle number, but a continued increase in O_3. The meteorology and nightime increase in O_3 is suggestive of a transported continental aged air mass arriving at Cape Grim, rather than local production. The average particle size distribution over this period (Fig. 4b) is a single broad distribution with a dominant mode of around 60 nm, and is similar in shape to the distribution during the particle growth event.

Period D. A strong urban influence is visible in the early morning on the 17 February (Fig. 3), when air is transported directly from metropolitan region of Melbourne

~ 300 km directly to the north (Fig. S1d). O_3 peaks at ~ 30 ppb, accompanied by particle number concentrations of similar magnitude to the direct BB plume the previous day, but without the elevated CO or BC. The significant urban influence is confirmed by a peak in HFC-134a, an urban tracer which is widely used in motor vehicle air conditioning and domestic refrigeration (McCulloch et al., 2003). The average particle size distribution (Fig. 4b) shows a single broad distribution with a dominant mode of 90 nm.

Period E. In mid afternoon on the 17 February a westerly wind from the ocean sector leads to a sudden drop in HFC-134a, O_3 and particle number. HYSPLIT trajectories suggest the air mass passed over the ocean for at least 60 h prior to arriving at Cape Grim (Fig. S1e). The particle size distribution changes from uni-modal to bi-modal, with dominant modes at around 50 and 160 nm (Fig. 4c). This bi-modal distribution is typical of clean marine air and aerosols are likely dominated by non sea salt (nss) sulphate and sea salt particles, which in the larger mode have been cloud processed (Lawler et al., 2014; Cravigan et al., 2015).

Period F. At midnight on the 18 February, (Fig. 3) terrestrial influence from mainland Australia is visible (Fig. S1f), with an increase in O_3, HFC-134a, and possible a particle growth event between 00:00–03:00 AEST, though the increase in particle diameter is more likely due to an influx of larger particles. Over the next 24 h, decreasing O_3 and particle number suggests the air is becoming increasingly free of terrestrial influence. However the HYSPLIT trajectory (Fig. S1f) shows that some terrestrial influence from mainland Australia remains for the next 24 h. This is also shown by HFC-134a values which are slightly higher than during clean marine period (event E), and a uni-model average particle size distribution (Fig. 4c), which resembles the terrestrially-influenced distributions corresponding to periods B, C, D and F.

It is interesting to note that while size distributions have been described as uni-modal for periods B, C, D and F, Fig. 4a–c shows evidence of a second minor mode at around 160–170 nm in each of these terrestrially-influenced periods. Due to the strong marine influence of the air arriving at Cape Grim, the 160–170 nm mode in these periods can likely be attributed to cloud processed nss sulphate and sea salt aerosol, and

corresponds to the second larger mode (160 nm) in the clean marine period of Fig. 3 period E.

3.1.2 Inferring chemical composition in BB event 1 (BB1) from CCN measurements

The ability of particles to act as CCN at 0.5 % supersaturation was investigated during the fresh BB plume (Fig. 3 period A) and the particle growth period (period B). The CCN activity of particles was also calculated during the 24 h of period F, chosen due to the absence of BB tracers during this period, and predominance of marine air with some minor terrestrial influence. The average hourly ratio of CCN number to condensation nuclei (CN) number > 80 nm (CN80, measured using the SMPS) was calculated. CN80 was chosen based on a study by Petter et al. (2009) which suggested even weakly hygroscopic BB aerosols began to activate to CCN at a diameter of approximately 80 nm and larger. Given this, any observed difference in the CCN / CN80 ratio may then be due to either different chemical composition between the particles, and/or differences in particles size distributions, as larger particles are more easily activated to CCN. The CCN / CN80 ratio has only been calculated for BB1 because there are no aerosol size distribution measurements (and hence no CN80 measurements) for BB2. The CCN / CN ratio for total CN measured with SMPS (CN > 14 nm) was also calculated.

Figure 5a shows the CCN / CN80 expressed as a percentage for the fresh plume (period A), particle growth event (period B), and background marine/terrestrial (period F). Error bars are ±1 standard error of the mean. Figure 5b shows the absolute number concentration of CCN during these periods.

The CCN / CN80 ratio is lowest during the fresh BB plume strike (period A) (56±8 %), and is substantially higher during the particle growth event (period B) (77 ± 4 %). For comparison, the CCN / total CN ratio for the fresh BB plume strike is 37 % (not shown). Figure 4a shows that the average dominant diameter of particles shifts from around 120 nm during period A to around 60 nm during the period B. The smaller diameter dur-

ing period B suggests that particle size is not the reason for the increased CCN / CN80 ratio during the particle growth period, but is likely due to a changing chemical composition of particles between the two periods, with more hygroscopic particle measured during the particle growth period compared to the fresh BB particles. As discussed above, an elevation of BC above typical background levels suggests dilute BB emissions are still present during this period. The changing chemical composition then is likely due to both a change in the source of particles (with a diminished BB influence and implied stronger marine inflence during period B) but also possibly the change in properties of the diluted BB particles. The increase in CCN / CN80 ratio during period B and implied increased hygroscopicity, alongside the particle growth event suggests a coating of particles with a material more hygroscopic than the primary particle.

Volatility and hygroscopicity measurements of particles are available from period A (Fletcher et al., 2007). These measurements suggested that 60 nm particles consisted of a non-hygroscopic 23 nm core, a hygroscopic layer to 50 nm and a hydrophobic outer layer to 60 nm (possible homogeneously mixed). There was some evidence that the particle core contained two different types of particle, possibly due to merging of marine and BB particles. The suggested mix of hygroscopic and non-hygroscopic materials in fresh BB particles is in agreement with the fact that only 56 % of these particles were hygroscopic enough to act as CCN. Unfortunately no hygroscopicity or volatility measurements are available from period B (particle growth).

During background marine period F, all (104 ± 3 %) of the particles > 80 nm could act as CCN (Fig. 5a). A value of more than 100 % is not physically possible but is due to uncertainty associated with the different techniques (SMPS and CCN) and measurement synchronisation. This result is in agreement with the work of Fletcher et al. (2007) who reported that the fresh BB particles from BB1 had a lower hygroscopic growth factor than marine particles. Figure 4a and c shows the average size distribution of particles during period F (background marine/terrestrial) is very similar to period B (particle growth), despite the air masses coming from different directions (westerly and easterly respectively). As discussed previously, both these periods have a predominent marine

back trajectory and some terrestrial influence. It is therefore likely that the main difference between the particle composition between these two periods, and the reason for the lower CCN / CN ratio during period B is the presence of non or weakly-hygroscopic > 80 nm particles from the recent BB emissions.

Sea salt and nss sulphate aerosol are important sources of CCN in the marine boundary layer (Korhonen et al., 2008; Quinn and Bates, 2011) and are likely the main source of CCN in period F (and possibly period B). The fact that all particles > 80 nm could act as CCN in period F suggests that any non-hygroscopic terrestrial particles which reached Cape Grim during this time were likely to have been aged and oxidised during the several hundred kms during transport from the mainland.

Finally, the hourly average of CCN number in the fresh plume (A) was $\sim 2000\,\mathrm{cm}^{-3}$ (Fig. 5b), with minute average concentrations up to $\sim 5500\,\mathrm{CCN\,cm}^{-3}$. In contrast, the average number of CCN during particle growth (period B) was a factor of 3 lower at $\sim 700\,\mathrm{CCN\,cm}^{-3}$, the decrease driven by dilution of the fresh smoke plume. During the background marine/terrestrial period (F) in BB1, the CCN is $320\,\mathrm{CCN\,cm}^{-3}$, with low variability, a value which is within the range of typical pristine marine values (Gras, 2007). Overall, CCN were enhanced by a factor ~ 6 and a factor of ~ 30 above background levels in BB1 and BB2 respectively (see Sect. 3.2 and Table 3). Despite the modest ability of fresh BB particles to form CCN (CCN / CN80 ratio of 56 %), the very high numbers of particles ejected into the marine boundary layer during the fire highlights the dramatic impact BB plumes can have on the CCN population, particularly in clean marine regions.

3.1.3 Discussion – determining drivers of ozone, particle growth and change in CCN / CN ratio in BB event 1 (BB1)

Of interest is the contribution that the BB emissions from the Robbins Island fire had on the particle growth event, and O_3 enhancement (Fig. 3). Determining the contribution from just one source is challenging given (a) the variety of emission sources impacting Cape Grim during during BB1 (BB, terrestrial, marine, urban), and understanding the

transport and mixing of these emissions (b) the complexity of chemistry involved in particle growth processes including gas to aersosol phase transfer, and of O_3 production and (c) the lack of specific BB tracers, such as levoglucosan and acetonitrile during this event (BC is a BB tracer but may also come from other combustion processes eg fossil fuel combustion). Similarly, without aerosol composition measurements, the changing composition of the particles during growth, and therefore the species responsible, cannot be determined.

Several studies have reported a larger diameter of particles in aged, diluted BB plumes compared to fresh BB plumes, due to coating of primary BB particles with low volatility organic and inorganic compounds (Janhäll et al., 2010; Kondo et al., 2011; Sahu et al., 2012; Akagi et al., 2012). The importance of photochemical reactions in driving the oxidation and condensation processes were higlighted recently by Vakkari et al. (2014) who found that the degree of oxidation and diameter was enhanced when the plume was transported in daylight hours compared to nightime. Rather fewer studies have reported size distributions for individual particle growth events in BB plumes as reported here. Particle nucleation and subsequent growth in fresh BB plumes occured in chamber studies with rapid growth rates of $12\,nm\,h^{-1}$ (Hennigan et al., 2012), which is approximately twice the growth rate observed in this study. In summary, there is evidence elswhere that particle diameter increases with BB plume dilution and aging, particularly during daylight hours.

Similarly the sources and chemical drivers of the change in CCN / CN80 ratio during the fresh plume and particle growth period are difficult to determine from observations alone. As discussed above the dominant mode diameter of particles during the particle growth event was smaller than during the fresh plume and so a change in particle composition leading to enhanced hygroscopicity is the likely driver of the enhanced ratio during particle growth. Chamber studies have shown that primary BB particles become more hygroscopic when coated with inorganics and oxygenated secondary organics (Martin et al., 2013; Petters et al., 2009; Engelhart et al., 2012). The increase in O_3 alongside the particle growth event indicates photochemical processing of the

Title Page

Abstract | Introduction

Conclusions | References

Tables | Figures

◀ | ▶

◀ | ▶

Back | Close

Full Screen / Esc

Printer-friendly Version

Interactive Discussion

diluted plume, which produce lower volatility organics and inorganics. However it is difficult to elucidate the mechanisms contributing to an increase in hygroscopicity when particles from the BB plume are externally mixed with particles and trace gases from a range of others sources.

⁵ Ozone production has been frequently reported in air impacted by BB, and there is some evidence of larger enhancements in air impacted by both BB and urban emissions (Jaffe and Wigder, 2012; Wigder et al., 2013). In BB1, the HFC-134a indicates an increasing influence from urban air from mainland Australia (indicating a likely source of O_3 or O_3 precursors), and indeed the O_3 and HFC-134a concentrations do increase ¹⁰ in parallel (Fig. 3). However, some of the increases in O_3 occured when there was minimal urban influence, for example during the particle growth event (Fig. 3 period B), and may have been driven by emissions from the local fire.

Use of a chemical transport model to determine the sources driving the particle growth, change in CCN / CN ratio and O_3 formation will be reported in a follow up ¹⁵ paper by Lawson et al. (2015).

3.2 BB event 2 (BB2) 23 February 2006

3.2.1 Interplay between emissions, meteorology and sources

BB2 was of much longer duration than BB1, and lasted about 29 h. Figure 6 shows a time series including wind direction and rainfall, O_3, CO, BC, BB tracer acetonitrile, ²⁰ acetonitrile / CO ratio (where CO > 400 ppb) and urban tracer HFC-134a. Periods of interest are highlighted as A–D (Fig. 6), summarised in Table 2 and discussed below. Particle size distribution data is not available for BB2. The matching air mass back trajectories for the events highlighted in Fig. 6 are shown in Fig. S2a–d.

Period A. For the first 24 h of BB2, there is clear elevation in CO, BC and acetonitrile, ²⁵ due to the easterly wind advecting the plume directly to Cape Grim. The acetonitrile mixing ratio is ∼ 1 ppb and is enhanced by a factor of 30 above typical background levels at Cape Grim of ∼ 35 ppt (Table 3). The acetonitrile ratio to CO is also relatively

constant during this time (1–2 ppt ppb^{-1}). An ozone peak of 27 ppb (minutely) occurs in mid afternoon on 24 February, corresponding to an hourly Normalised Excess Mixing Ratio (NEMR) $\Delta O_3 / \Delta CO$ of 0.05 (where NEMR is an excess mixing ratio normalised to a non-reactive co-emitted tracer, in this case CO, see Akagi et al., 2011).

5   Period B. At 04:00 AEST on 25 February acetonitrile peaks by a factor of 17 over 2 h (Fig. 6 period B) with a smaller peak at 23:00 AEST on the 24 February (factor of 5 increase). Almost all masses on the PTR-MS increased at the same time as acetonitrile, including masses corresponding to HCN, methanol, acetaldehyde, acetone, furan/isoprene and benzene which increased by a factor of 3–5 during the first peak
10   at 23:00 AEST and a factor of 6–16 during the second peak at 04:00 AEST (hourly average values). The corresponding CO peak at 04:00 AEST ($\sim$ 1500 ppb) increased by a factor of 21 over 2 h and is the largest peak from BB2. While BC has a corresponding peak at 04:00 AEST (factor of 5 increase) this BC peak is much smaller than peaks which occured earlier in BB2. CN number showed an increase in concentration
15   by a factor of 4 during peak 1 and factor of 7 during peak 2. This large enhancement in CO and NMOCs but modest enhancement in BC suggests a decrease in the combustion efficiency during this time. This is further supported by increases in the ratio of acetonitrile to CO (where CO > 400 ppb) by a factor of $\sim$ 3 during the peak periods (Fig. 6), and a decrease in the ratios of BC to CO during peak periods (average
20   0.9 ± 0.3 ng m^{-3} ppb^{-1}) compared to non-peak periods (2.2 ± 0.1 ng m^{-3} ppb^{-1}).

A small amount of rainfall recorded at Cape Grim (1.4 mm) corresponds with the second peak (Fig. 6). Archived radar images from the Bureau of Meteorology (West Takone 128 km, 10 min resolution) confirm that at very light patchy rain showers occured on Robbins Island at 23:10 AEST followed by intermittent rain showers of light
25   to moderate intensity from 12:40 AEST until 05:40 AEST, on the 25 February (S. Baly, personal communication, 2015). The total rainfal amount that fell on Robbins Island was between 1–5 mm (www.bom.gov.au). Evidence of rainfall coinciding with an enhancement in NMOC ER to CO, and a decrease in BC ER to CO suggests that the rainfall changed the combustion dynamics of the fire. The enhanced mixing ratios of

NMOCs and CO which are associated with low-efficiency, smouldering combustion, can therefore attributed to a short term enhancement in emissions, driven by rainfall. Due to the small number of data points (2) it is not possible to calculate reliable ER to CO during this shortlived event.

While the elevated concentrations of BB tracers CO, BC and acetonitrile during this period are attributed to emissions from the local fire, back trajectories (Fig. S3b) show that during this period air arriving at Cape Grim had previously passed over the Australian mainland. The increasing anthropogenic influence is also supported by increasing levels of HFC-134a and a corresponding increase in O_3 which peaks at 34 ppb (minutely) at 01:00–02:00 AEST, with an hourly NEMR for ΔO_3 / ΔCO of 0.07 (the highest observed).

Period C. With a change in wind direction further to the north from 05:00 AEST onwards (Fig. 6), BB tracers BC, CO and acetonitrile all decrease to background levels, suggesting fire emissions are no longer impacting the station. Ozone begins to increase at 08:00 AEST and reaches ~ 40 ppb 3 h later, corresponding with a maximum HFC-134a mixing ratio of ~ 35 ppt. The air mass back trajectory (Fig. S2c) confirms that air from Melbourne impacting the station during this period.

Period D. As wind moves further to the west in to the clean marine sector (Fig. S2d), O_3 and HFC-134a decrease to background levels.

This time series highlights possible interplay of sources and meteorology on the observed trace gases. The very large increase of NMOCs and CO observed during the rainfall period shows the potentially large affect of quite minor meteorological events on BB emissions. While other studies have found a link between fuel moisture, MCE and emissions of $PM_{2.5}$, (e.g. Watson et al., 2011; Hosseini et al., 2013) this is the first study to our knowledge which has linked rainfall with a large increase in trace gas emissions from BB.

This work also highlights the large influence that BB plumes can have on the composition of the background atmosphere. During the direct plume strikes, absolute numbers of particles > 3 nm increased from 600 to 25 000 particles cm^{-3} (hourly average).

These particle number concentrations are in good agreement with ground-based mea-surements at background sites in the Amazon (20 000 particles cm^{-3}) (Artaxo et al., 2013) and at a forested site in Finland (30 000 particles cm^{-3}) (Virkkula et al., 2014). The absolute number of CCN increased from 160 particles cm^{-3} in background air up to 5500 particles cm^{-3} in BB2, a factor of 34 increase, in agreement with a study who showed a dry season increase in CCN of a factor 10–20 in the Amazon, attributed to BB aerosols (Andreae et al., 2002). In BB2, as was the case in BB1, the O_3 concentrations closely correspond with the HFC134a concentrations. This suggests that transport of photochemically processed air from urban areas to Cape Grim is the main driver of the O_3 observed but does not rule out possible local O_3 formation from BB emissions. NEMRs of ΔO$_3$ / ΔCO ranged from 0.001–0.074 during BB2 which are comparable to NEMRs observed elsewhere in BB plumes < 1 h old (Yokelson et al., 2003, 2009).

3.2.2 Chemical composition of BB2 and selection of in-plume and background periods

The composition of the fresh plume during BB2 was explored by determining for which trace gas and aerosol species the enhancement above background concentrations was statistically significant. Emission ratios (ER) to CO were then calculated for these selected species and converted to emission factors (EF).

The first 10 h of period A from BB2 (from 23:00 AEST on the 23 February to 09:00 AEST on the 24 February) was selected to characterise the fresh plume compo-sition. During this time, the air which brought the Robbins Island BB emissions to Cape Grim had previously passed over the ocean and so was free of terrestrial or urban in-fluence (NOAA HYSPLIT Fig. S2a). While fresh BB emissions were measured at Cape Grim beyond 10:00 AEST on the 24 February, the air at this time had prior contact with the Australian mainland, including the Melbourne region and so was considered unsuit-able for characterising the BB plume. During the selected time period, wind speeds of 16 m s^{-1} meant that the plume travelled the 20 km to Cape Grim over a period of about 20 min, which allows the plume to cool to ambient temperatures but ensures minimum

photochemical processing of the plume (Akagi et al., 2011). Advection of the plume to the site occurred primarily at night so minimal impact of photochemical reactions on the plume composition is expected (Vakkari et al., 2014). Finally, photos indicate the Robbins Island fire plume was well mixed within the boundary layer and was not lofted into the FT, allowing representative "fire-averaged" measurements to be collected (Akagi et al., 2014).

Background concentrations of gas and particle species were determined from fire-free periods in early March 2006 which had a very similar air back trajectory to trajectories during the fire (not shown). Concentrations of long lived urban tracers (not emitted from fires) including HFC-32, HFC-125a and HFC-134a were also used to match suitable background time periods with the fresh plume period.

Table 3 lists the gas and aerosol species measured, whether concentrations were statistically higher in the plume compared to background air, average background concentrations, average in-plume concentrations, emission ratios (ER) to CO and EF $(g\,kg^{-1})$. Details of ER and EF calculations are given below. Hourly average data were used for these calculations.

3.2.3 Species emitted in BB event 2 (BB2) – t tests

Hypothesis testing using the student t tests (one sided) were carried out to determine whether concentrations in the BB plume (x_1) were significantly higher than concentrations observed in the background periods (x_2), with a 95 % level of significance. Table 3 shows which species were statistically enhanced in the BB plume, and hence assumed to be emitted from the fire ($x_1 - x_2 > 0$) and those which were not statistically enhanced in the BB plume ($x_1 - x_2 = 0$). While the vast majority of species measured were found to be significantly enhanced in the BB plume, there were a number of species including DMS, chloroform, methyl chloroform, dichloromethane, carbon tetrachloride, bromoform and the urban tracers HFC-032, HFC-125 and HFC-134a which were not significantly enhanced. DMS has consistently been found to be emitted from BB in many studies (as summarised by Akagi et al., 2011). However, in this study due to close prox-

imity to the ocean, the likely emission of DMS from the BB was likely obscured by the high variability in the background concentration. The absence of emission of chloroform, methyl chloroform, dichloromethane, carbon tetrachloride, tribromomethane and the HFCs are in agreement with a recent study of boreal forest emissions by Simpson et al. (2011).

3.2.4 Calculation of emission ratios to CO

Excess mixing ratios (Δx) were calculated for species that were statistically higher in the plume compared to background air by subtracting background mixing ratios from the hourly in-plume mixing ratios. Emission ratios to CO were then calculated by plotting Δx vs. ΔCO, fitting a least squares line to the slope and forcing the intercept to zero (Yokelson et al., 1999). Emission (ER) to CO and the R^2 of the fit are reported in Table 3. The excess mixing ratios of all species significantly enhanced in the plume correlated with the excess mixing ratios of CO with an R^2 value of ≥ 0.4, with the exception of CO_2, HCHO, HCOOH, m/z 101, N_2O, and CCN number concentration (see discussion below and Table 3).

ER plots for BC, CN > 3 nm, H_2, CH_4, C_2H_6, C_6H_6, CH_3COOH, C_6H_6O and C_2H_3N are shown in Fig. 7. The ER of CO to particle number ($38\,\mathrm{cm^{-3}\,ppb^{-1}}$) agrees well with a literature averaged value of $34 \pm 16\,\mathrm{cm^{-3}\,ppb^{-1}}$ (Janhall et al., 2010). The H_2 ER to CO (0.10) is lower than the range reported from BB emissions (0.15–0.45), as summarised by Vollmer et al. (2012). The ER of BC to CO ($2.8\,\mathrm{ng\,m^{-3}\,ppb^{-1}}$) is similar to that derived for smouldering fires of $2.3 \pm 2.2\,\mathrm{ng\,m^{-3}\,ppbv^{-1}}$ (Kondo et al., 2011), where ppbv is approximately equal to molar ppb used here.

There is a low correlation between mixing ratios of CO and CO_2 (ER to CO $R^2 = 0.15$, see Table 3). This is likely because the enhancement of CO_2 in BB plumes is very small compared to the variation of CO_2 in the background atmosphere, particularly when sampling at some distance from the fire (Andreae et al., 2012). The lack of correlation seen here between CO and CO_2 means that the CO_2 emissions from the fire

cannot be reliably determined. For this reason, in Sect. 3.2.5., EFs are calculated using a published EF for CO.

Of the other species with R^2 values of < 0.4, HCHO and HCOOH are both emitted directly from BB, but are also oxidation products of other species co-emitted in BB. It is therefore possible that in the 20 min period between plume generation and sampling, chemical processing has lead to generation of these compounds in the plume, which has changed the ER to CO. In addition, sampling losses of HCOOH down the inlet line are possible as observed by Christian et al. (2004). The lack of relationship between ΔCO and ΔN_2O is likely because N_2O is an intermediate oxidation product which is both formed and destroyed during combustion. Studies of emissions from Savanna burning in Northern Australia have found N_2O to be insensitive to changes in MCE (Meyer and Cook, 2015; Meyer et al., 2012; Volkova et al., 2014). A further reason for a lack of correlation with ΔCO for ΔN_2O is that as for CO_2, the plume enhancement of ΔN_2O is relatively small compared to the observed variability in background concentrations. Finally the lack of correlation between ΔCCN and ΔCO may be due interaction of plume aerosol with background sources of CCN, such as sea salt, and the change in particle properties and composition in the 20 min after emission.

3.2.5 Calculation of EF and comparison with other studies

EFs ($g \, kg^{-1}$ fuel) were calculated using the equation detailed in Andreae et al. (2001), using CO as the reference gas:

$$EF(X) = ER(X/CO) \times \frac{MW(X)}{MW(CO)} \times EF(CO) \tag{1}$$

Where EF (X) is the calculated emission factor in $g \, kg^{-1}$ fuel, ER (X / CO) is the molar emission ratio with respect to CO, MW(X) is the molecular weight of the trace species, MW(CO) is the molecular weight of CO, and EF(CO) is the emission factor of CO. The EF(CO) used was the temperate average EF from Akagi et al. (2011) of $89 \pm 32 \, g \, CO \, kg^{-1}$ fuel, which corresponds to MCE of 0.92.

EFs were calculated only for species which had an ER with CO with a fit of $R^2 > 0.4$ (which excludes HCHO, HCOOH and N_2O) and were statistically emitted from the fire according to the t test (see Table 3). As the EFs calculated were from a single fire, no variability (e.g. standard deviation) is given.

Table 4 shows EFs calculated from this study compared with other Australian BB studies both of eucalypt and schlerophyll forest fires in temperate south eastern Australia (Paton-Walsh et al., 2005, 2008, 2014), and tropical savanna fires in northern Australia (Paton-Walsh et al., 2010; Meyer et al., 2012; Hurst et al., 1994a, 1994b; Shirai et al., 2003; Smith et al., 2014). The fire in this study (41° S) is > 1000 km south of the temperate forest fires used for comparison (33–35° S), and some 2500 km South East of the tropical savannah fires in the comparison (12–14° S). The vegetation in this study (coastal scrub and grasses) is comparable in structure to the mid and lower story vegetation in the temperate forest and savannah woodland fires in the other Australian studies, though lacks the coarse woody debris and the dominant upper story of trees found particularly in temperate Australian forests.

Two of the temperate Australian studies (Paton-Walsh et al., 2005, 2008) use a published EF for CO (Andreae and Merlet (2001) extra tropical value of 107 g kg^{-1}), to convert ER to EF while the temperate study by Paton Walsh et al. (2014) measured a CO emission factor of 118 g kg^{-1}. These CO EF from Paton-Walsh et al. (2005, 2008, 2014) correspond to MCEs ranging between 0.88–0.91, slightly lower than the MCE assumed here of 0.92. The Australian savanna studies used for comparison all measured CO and CO_2 EF corresponding to a MCE of 0.92. EFs from temperate vegetation in the NH are also included for comparison: Akagi et al. (2011) reports average EFs for temperate pine-oak, evergreen and coniferous forests (average MCE 0.92), and Yokelson et al. (2013) gives an average EF for temperate semi arid shrub land including coastal sage scrub and maritime chaparral (MCE 0.94). The vegetation burned in Yokelson et al. (2013) is expected to be more similar in structure to the Robbins Island coastal scrub than the temperate forests in Akagi et al. (2011).

For most species, there is a good agreement between EFs from this study and EFs previously published from Australia and elsewhere. The H_2 EF from this study (0.64 g kg^{-1}) is approximately one third the EF from Akagi et al. (2011) (2.03 g kg^{-1}), however there is a large variability reported in the Akagi et al. (2011) average value. There are no previously reported H_2 EFs for Australia. The CH_4 EF from this study (2.49 g kg^{-1}) is slightly higher than EF for the tropical savanna studies (2.03–2.33 g kg^{-1}). The C_2H_6 EF reported here of 0.30 g kg^{-1} agrees very closely with the SE Australian EF by Paton-Walsh et al. (2005) (0.26 g kg^{-1}), and is lower than (but within variability of) the value reported by Paton-Walsh et al. (2014) of 0.5 g kg^{-1}. The ethane EF reported here (0.3 g kg^{-1}) is within the wide range reported from Australian savanna burns (0.08–0.6 g kg^{-1}), and a factor of almost a factor of 4 lower than the NH temperate forests average (Akagi et al., 2011) although comparable to coastal scrub and chaparral (Yokelson et al., 2013).

The HCN EF (0.49 g kg^{-1}) agrees well with the temperate SE Australian value of 0.43 g kg^{-1} (Paton-Walsh et al., 2005) and is at the higher end of the wide range reported for tropical Australian savanna (0.11–0.53 g kg^{-1}). The HCN EF reported here is lower than values from the NH temperate forests (0.73 g kg^{-1}) and coastal scrub and chaparral (0.75 g kg^{-1}). There are no temperate Australian acetonitrile EFs available for comparison, but the EF from this study (0.17 g kg^{-1}) agrees well with that from the Australian savanna (0.11 g kg^{-1}) and temperate coastal scrub and chaparral (0.15 g kg^{-1}). No Australian EF for phenol is available for comparison but the EF from this study (0.24 g kg^{-1}) is somewhat lower to those reported in the temperate NH by Akagi et al. (2011) (0.33 g kg^{-1}) and Yokelson (0.45 g kg^{-1}). Acetic acid EF from this study (0.52 g kg^{-1}) is a factor of 7 lower than temperate value by Paton-Walsh et al. (2014) (3.8 g kg^{-1}), and a factor of 4 lower than those reported in the temperate NH by Akagi et al. (2011) (1.97 g kg^{-1}) and Yokelson et al. (2013) (1.91 g kg^{-1}) though the variability in these values is large. The methanol EF (1.37 g kg^{-1}) is somewhat lower than temperate EF of 2.03 and 2.4 g kg^{-1} (Paton-Walsh et al., 2005, 2014) and 1.93 g kg^{-1},(Akagi et al., 2011) though agrees very well with Yokelson et al. (2013) EF of 1.35 g kg^{-1}.

The EF for benzene ($0.47\,\mathrm{g\,kg^{-1}}$) is in the upper range reported for Australian savanna burning by Hurst et al. (1994a, b) (0.29–$0.42\,\mathrm{g\,kg^{-1}}$), is higher than Shirai et al. (2003) savanna ($0.21\,\mathrm{g\,kg^{-1}}$) and agrees closely with the Yokelson et al. (2013) temperate value of $0.45\,\mathrm{g\,kg^{-1}}$. The toluene EF ($0.17\,\mathrm{g\,kg^{-1}}$) has no Australian EF for comparison but is similar to the temperate value reported by Yokelson et al. (2013) ($0.20\,\mathrm{g\,kg^{-1}}$).

While the EF for the methyl halides here are in the same proportion as other studies (e.g. $EF(CH_3Cl) > EF(CH_3Br) > EF(CH_3I)$), the magnitude of the EF are substantially higher than other studies. The CH_3Cl EF from this study ($0.208\,\mathrm{g\,kg^{-1}}$) is more than a factor of 3 higher than elsewhere in Australia and the NH, the EF of CH_3Br between 4 and 9 times higher and CH_3I a factor of about 2 times higher than elsewhere. The ER to CO correlation for the methyl halides on which these EF are based consists of only a few observations. However, the ethane (C_2H_6) ER to CO and EF in this study was derived from the same number of data points and same measurement system (the AGAGE CGMS Medusa), and the resulting EF for C_2H_6 is very consistent with other EF from Australian temperate and savanna regions, as discussed above. It is therefore possible that the high methyl halide EFs reported here are due to high halogen content of soil and vegetation on the island, due to very close proximity to the ocean, and transfer of halogens to the soil via sea spray. Chlorine content in vegetation does vary substantially as reported by Lobert et al. (1999) and Christian et al. (2003) but whether a high halogen content in vegetation is the reason for these high EF remains unknown. A further reason could be a contribution from another local source; while the methyl halide emission ratios were calculated using background mixing ratios similar to multi-annual average Cape Grim mixing ratios in air from NW Tasmania, elevated methyl halide "events" have been previously linked to coastal wetlands around and to the east of Robbins Island (Cox et al., 2005, 2003).

In summary, the EF reported for this study agree well with other EF from temperate Australia with the exception of acetic acid. These temperate EF (with the exception of acetic acid and ethane) are higher than or in the upper range of Tropical Australian savannah EF. Compared to NH temperate EF, most species in this study have EF lower

than reported in Akagi et al. (2011) NH temperate forests, despite the fact that EF in this study were calculated using the CO EF from Akagi et al. (2011) and therefore assumes the same MCE. The values from this study are in many cases in very good agreement with the NH coastal scrub and chaparral values reported by Yokelson et al. (2013), particularly for ethane, HCN, acetaldehyde, methanol, benzene and toluene.

4   Conclusions and future work

The opportunistic measurement of BB plumes at Cape Grim Baseline Air Pollution Station in February 2006 has allowed characterisation of BB plumes in a region with few BB measurements. Plumes were measured on two occasions (events BB1 and BB2) when the plume was advected to Cape Grim from a fire on Robbins Island some 20 km to the east.

The fresh plume had a large impact on the number of particles at Cape Grim, with absolute numbers of particles > 3 nm increasing from 600 cm^{-3} in background air up to 25 000 cm^{-3} during the fresh plume in BB2 (hourly average) and CCN increasing from 160 cm^{-3} in background air up to 5500 cm^{-3} (hourly average). The dominant particle diameter mode was 120 nm during the fresh plume.

During BB1, dilution of the plume in the morning via a wind direction change resulted in a drop in the dominant particle mode to 50 nm, and a particle growth event in which particles grew to 80 nm over 5 h. Particle growth was accompanied by an increase in O_3 from 12 to 20 ppb, suggesting photochemical processing of air and condensation of low volatility oxidation products may be driving the particle growth. During BB1, the ability of particles > 80 nm to act as CCN at 0.5 % supersaturation was investigated, including during the fresh BB, particle growth and background terrestrial/marine periods. The ΔCCN / ΔCN80 ratio was lowest during the fresh BB plume strike (57 %), higher during the particle growth event (77 %) and is higher still (104 %) in background marine air.

Without chemical composition measurements, it is difficult to determine the sources, and the chemical species responsible for the particle growth event, and the increase in

CCN / CN80 ratio observed during BB1. The implied increase in hygroscopicity during the particle growth period, along with an increase in particle diameter is suggestive of condensation of a hygroscopic coating, such as inorganics or highly oxidised organics, on primary particles of low hygroscopicity. However, identities of the condensing species, and the source of trace gases and aerosols during this period are difficult to determine with observations alone.

Enhancements in O_3 concentration above background were observed following the direct plume strikes in BB1 and during the direct plume strike in BB2, with NEMRs ($\Delta O_3 / \Delta CO$) of 0.001–0.074. It is likely that some of the O_3 enhancement that occured during the particle growth event in BB1 was driven by fire emissions. However on other occasions enhancement of O_3 which occured at night, corresponding with enhancements of urban tracer HFC-134a was most likely due to air being transported from mainland Australia. Chemical transport modelling will be used in a follow up paper to elucidate the sources, and where possible the species responsible for the O_3 enhancement, particle growth and change in particle hygroscopicity observed.

The more prolonged BB2 allowed determination of emission ratios (ER) to CO for a range of trace gas species, CN and BC, and these have been used to determine emission factors in g kg^{-1} of fuel. While these EF are based on only one fire and were calculated using a published EF for CO (an average temperate value), this work provides new estimates of EFs for a number of trace gas species for burning of coastal scrubland in temperate Australia.

A very large increase in emissions of NMOCs (factor of 16) and CO (factor of 21), and a more modest increase in BC (factor of 5) occurred during BB2. The ratio of acetonitrile to CO increased by a factor of 2–3 and the ratio of BC to CO halved during this period. This change in emissions and ratios is attributed to decreased combustion efficiency during this time, due to rainfall over Robbins Island. Given that air quality and climate models typically use a fixed EF for trace gas and aerosol species, the impact of varying emissions due to meteorology may not be captured by models.

Full Screen / Esc

Printer-friendly Version

Interactive Discussion

More broadly, given the high variability in reported EF for trace gas and aerosol species in the literature, the impact of EF variability on modelled outputs of both primary BB species (i.e CO, BC, NMOCs) and secondary BB species (i.e O_3, oxygenated NMOCs, secondary aerosol) is likely to be significant. However, few studies have systematically examined the impact of EF variability on model outputs. In the next phase of this work, in addition to exploring the chemistry described above with chemical transport modelling, we will also systematically explore the sensitivity of these models to EF variability, as well as spatial and meteorological variability.

The Supplement related to this article is available online at doi:10.5194/acpd-15-17599-2015-supplement.

References

Akagi, S. K., Yokelson, R. J., Wiedinmyer, C., Alvarado, M. J., Reid, J. S., Karl, T., Crounse, J. D., and Wennberg, P. O.: Emission factors for open and domestic biomass burning for use in atmospheric models, Atmos. Chem. Phys., 11, 4039–4072, doi:10.5194/acp-11-4039-2011, 2011.

Akagi, S. K., Craven, J. S., Taylor, J. W., McMeeking, G. R., Yokelson, R. J., Burling, I. R., Urbanski, S. P., Wold, C. E., Seinfeld, J. H., Coe, H., Alvarado, M. J., and Weise, D. R.: Evolution of trace gases and particles emitted by a chaparral fire in California, Atmos. Chem. Phys., 12, 1397–1421, doi:10.5194/acp-12-1397-2012, 2012.

Akagi, S. K., Burling, I. R., Mendoza, A., Johnson, T. J., Cameron, M., Griffith, D. W. T., Paton-Walsh, C., Weise, D. R., Reardon, J., and Yokelson, R. J.: Field measurements of trace gases emitted by prescribed fires in southeastern US pine forests using an open-path FTIR system, Atmos. Chem. Phys., 14, 199–215, doi:10.5194/acp-14-199-2014, 2014.

Andreae, M. O. and Merlet, P.: Emission of trace gases and aerosols from biomass burning, Global Biogeochem. Cy., 15, 955–966, doi:10.1029/2000gb001382, 2001.

Andreae, M. O., Artaxo, P., Brandao, C., Carswell, F. E., Ciccioli, P., da Costa, A. L., Culf, A. D., Esteves, J. L., Gash, J. H. C., Grace, J., Kabat, P., Lelieveld, J., Malhi, Y., Manzi, A. O., Meixner, F. X., Nobre, A. D., Nobre, C., Ruivo, M., Silva-Dias, M. A., Stefani, P., Valentini, R., von Jouanne, J., and Waterloo, M. J.: Biogeochemical cycling of carbon, water, energy, trace gases, and aerosols in Amazonia: the LBA-EUSTACH experiments, J. Geophys. Res.-Atmos., 107, 8066, doi:10.1029/2001jd000524, 2002.

Andreae, M. O., Artaxo, P., Beck, V., Bela, M., Freitas, S., Gerbig, C., Longo, K., Munger, J. W., Wiedemann, K. T., and Wofsy, S. C.: Carbon monoxide and related trace gases and aerosols over the Amazon Basin during the wet and dry seasons, Atmos. Chem. Phys., 12, 6041–6065, doi:10.5194/acp-12-6041-2012, 2012.

Artaxo, P., Rizzo, L. V., Brito, J. F., Barbosa, H. M. J., Arana, A., Sena, E. T., Cirino, G. G., Bastos, W., Martin, S. T., and Andreae, M. O.: Atmospheric aerosols in Amazonia and land use change: from natural biogenic to biomass burning conditions, Faraday Discuss., 165, 203–235, doi:10.1039/c3fd00052d, 2013.

Buckby, P.: Robbins Island Saga, The Commercial Finance Company of Tasmania Pty. Ltd., Smithton, Tasmania, 1988.

Cainey, J. M., Keywood, M., Grose, M. R., Krummel, P., Galbally, I. E., Johnston, P., Gillett, R. W., Meyer, M., Fraser, P., Steele, P., Harvey, M., Kreher, K., Stein, T., Ibrahim, O., Ristovski, Z. D., Johnson, G., Fletcher, C. A., Bigg, E. K., and Gras, J. L.: Precursors to Particles (P2P) at Cape Grim 2006: campaign overview, Environ. Chem., 4, 143–150, doi:10.1071/en07041, 2007.

Christian, T. J., Kleiss, B., Yokelson, R. J., Holzinger, R., Crutzen, P. J., Hao, W. M., Saharjo, B. H., and Ward, D. E.: Comprehensive laboratory measurements of biomass-burning

emissions: 1. emissions from Indonesian, African, and other fuels, J. Geophys. Res.-Atmos., 108, 4719, doi:10.1029/2003jd003704, 2003.

Christian, T. J., Kleiss, B., Yokelson, R. J., Holzinger, R., Crutzen, P. J., Hao, W. M., Shirai, T., and Blake, D. R.: Comprehensive laboratory measurements of biomass-burning emissions: 2. first intercomparison of open-path FTIR, PTR-MS, and GC-MS/FID/ECD, J. Geophys. Res.-Atmos., 109, D02311, doi:10.1029/2003jd003874, 2004.

Cox, M. L., Sturrock, G. A., Fraser, P. J., Siems, S. T., Krummel, P. B., and O'Doherty, S.: Regional sources of methyl chloride, chloroform and dichloromethane identified from AGAGE observations at Cape Grim, Tasmania, 1998–2000, J. Atmos. Chem., 45, 79–99, doi:10.1023/A:1024022320985, 2003.

Cox, M. L., Sturrock, G. A., Fraser, P. J., Siems, S. T., and Krummel, P. B.: Identification of regional sources of methyl bromide and methyl iodide from AGAGE observations at Cape Grim, Tasmania, J. Atmos. Chem., 50, 59–77, doi:10.1007/s10874-005-2434-5, 2005.

Cravigan, L. T., Ristovski, Z., Modini, R. L., Keywood, M. D., and Gras, J. L.: Observation of sea salt fraction in sub-100 nm diameter particles at Cape Grim, J. Geophys. Res.-Atmos., 120, 1848–1864, doi:10.1002/2014JD022601, 2015.

Cubison, M. J., Ortega, A. M., Hayes, P. L., Farmer, D. K., Day, D., Lechner, M. J., Brune, W. H., Apel, E., Diskin, G. S., Fisher, J. A., Fuelberg, H. E., Hecobian, A., Knapp, D. J., Mikoviny, T., Riemer, D., Sachse, G. W., Sessions, W., Weber, R. J., Weinheimer, A. J., Wisthaler, A., and Jimenez, J. L.: Effects of aging on organic aerosol from open biomass burning smoke in aircraft and laboratory studies, Atmos. Chem. Phys., 11, 12049–12064, doi:10.5194/acp-11-12049-2011, 2011.

de Gouw, J. and Warneke, C.: Measurements of volatile organic compounds in the earths atmosphere using proton-transfer-reaction mass spectrometry, Mass Spectrom. Rev., 26, 223–257, doi:10.1002/mas.20119, 2007.

Dunne, E., Galbally, I. E., Lawson, S. J., and Patti, A.: Interference in the PTR-MS measurement of acetonitrile at m/z 42 in polluted urban air – a study using switchable reagent ion PTR-MS, Int. J. Mass Spectrom., 319–320, 40–47, doi:10.1016/j.ijms.2012.05.004, 2012.

Engelhart, G. J., Hennigan, C. J., Miracolo, M. A., Robinson, A. L., and Pandis, S. N.: Cloud condensation nuclei activity of fresh primary and aged biomass burning aerosol, Atmos. Chem. Phys., 12, 7285–7293, doi:10.5194/acp-12-7285-2012, 2012.

Ferek, R. J., Reid, J. S., Hobbs, P. V., Blake, D. R., and Liousse, C.: Emission factors of hydro-carbons, halocarbons, trace gases and particles from biomass burning in Brazil, J. Geophys. Res.-Atmos., 103, 32107–32118, doi:10.1029/98JD00692, 1998.

Fletcher, C. A., Johnson, G. R., Ristovski, Z. D., and Harvey, M.: Hygroscopic and volatile properties of marine aerosol observed at Cape Grim during the P2P campaign, Environ. Chem., 4, 162–171, doi:10.1071/en07011, 2007.

Galbally, I. E., Lawson, S. J., Weeks, I. A., Bentley, S. T., Gillett, R. W., Meyer, M., and Gold-stein, A. H.: Volatile organic compounds in marine air at Cape Grim, Australia, Environ. Chem., 4, 178–182, doi:10.1071/en07024, 2007a.

Galbally, I. E., Meyer, C. P., Bentley, S. T., Lawson, S. J., and Baly, S. B.: Reactive gases in near surface air at Cape Grim, in: 2005–2006 Baseline Atmospheric Program (Australia), edited by: Cainey, J. M., Derek, N., and Krummel, P. B., Australian Bureau of Meteorology and CSIRO Marine and Atmospheric Research, Melbourne, 77–79, available at: http://www.bom.gov.au/inside/cgbaps/baseline/Baseline_2005-2006.pdf (last access: 13 May 2015), 2007b.

Gras, J. L.: Particles program report, in: 2005–2006 Baseline Atmospheric Program (Australia), edited by: Cainey, J. M., Derek, N., and Krummel, P. B., Australian Bureau of Meteorology and CSIRO Marine and Atmospheric Research, Melbourne, 85–86, available at: http://www.bom.gov.au/inside/cgbaps/baseline/Baseline_2005-2006.pdf (last acccess: 13 May 2015), 2007.

Hecobian, A., Liu, Z., Hennigan, C. J., Huey, L. G., Jimenez, J. L., Cubison, M. J., Vay, S., Diskin, G. S., Sachse, G. W., Wisthaler, A., Mikoviny, T., Weinheimer, A. J., Liao, J., Knapp, D. J., Wennberg, P. O., Kürten, A., Crounse, J. D., Clair, J. St., Wang, Y., and We-ber, R. J.: Comparison of chemical characteristics of 495 biomass burning plumes inter-cepted by the NASA DC-8 aircraft during the ARCTAS/CARB-2008 field campaign, Atmos. Chem. Phys., 11, 13325–13337, doi:10.5194/acp-11-13325-2011, 2011.

Hennigan, C. J., Miracolo, M. A., Engelhart, G. J., May, A. A., Presto, A. A., Lee, T., Sulli-van, A. P., McMeeking, G. R., Coe, H., Wold, C. E., Hao, W.-M., Gilman, J. B., Kuster, W. C., de Gouw, J., Schichtel, B. A., Collett Jr., J. L., Kreidenweis, S. M., and Robinson, A. L.: Chemical and physical transformations of organic aerosol from the photo-oxidation of open biomass burning emissions in an environmental chamber, Atmos. Chem. Phys., 11, 7669–7686, doi:10.5194/acp-11-7669-2011, 2011.

Hennigan, C. J., Westervelt, D. M., Riipinen, I., Engelhart, G. J., Lee, T., Collett, J. L., Pan-dis, S. N., Adams, P. J., and Robinson, A. L.: New particle formation and growth in biomass

burning plumes: an important source of cloud condensation nuclei, Geophys. Res. Lett., 39, L09805, doi:10.1029/2012gl050930, 2012.

Hosseini, S., Urbanski, S. P., Dixit, P., Qi, L., Burling, I. R., Yokelson, R. J., Johnson, T. J., Shri-vastava, M., Jung, H. S., Weise, D. R., Miller, J. W., and Cocker, D. R.: Laboratory characteri-zation of PM emissions from combustion of wildland biomass fuels, J. Geophys. Res.-Atmos., 118, 9914–9929, doi:10.1002/jgrd.50481, 2013.

Hurst, D. F., Griffith, D. W. T., Carras, J. N., Williams, D. J., and Fraser, P. J.: Measurements of trace gases emitted by australian savanna fires during the 1990 dry season, J. Atmos. Chem., 18, 33–56, doi:10.1007/bf00694373, 1994a.

Hurst, D. F., Griffith, D. W. T., and Cook, G. D.: Trace gas emissions from biomass burning in tropical australian savannas, J. Geophys. Res.-Atmos., 99, 16441–16456, doi:10.1029/94jd00670, 1994b.

ISO: ISO 6879 Air Quality, Performance Characteristics and Related Concepts for Air Quality Measuring Methods, ISO, Geneva, 1995.

Inomata, S., Tanimoto, H., Kameyama, S., Tsunogai, U., Irie, H., Kanaya, Y., and Wang, Z.: Technical Note: Determination of formaldehyde mixing ratios in air with PTR-MS: laboratory experiments and field measurements, Atmos. Chem. Phys., 8, 273–284, doi:10.5194/acp-8-273-2008, 2008.

Jaffe, D. A. and Wigder, N. L.: Ozone production from wildfires: a critical review, Atmos. Environ., 51, 1–10, doi:10.1016/j.atmosenv.2011.11.063, 2012.

Janhäll, S., Andreae, M. O., and Pöschl, U.: Biomass burning aerosol emissions from vegetation fires: particle number and mass emission factors and size distributions, Atmos. Chem. Phys., 10, 1427–1439, doi:10.5194/acp-10-1427-2010, 2010.

Karl, M., Gross, A., Leck, C., and Pirjola, L.: Intercomparison of dimethylsulfide oxidation mech-anisms for the marine boundary layer: gaseous and particulate sulfur constituents, J. Geophys. Res.-Atmos., 112, D15304, doi:10.1029/2006jd007914, 2007.

Karl, T. G., Christian, T. J., Yokelson, R. J., Artaxo, P., Hao, W. M., and Guenther, A.: The Tropical Forest and Fire Emissions Experiment: method evaluation of volatile organic com-pound emissions measured by PTR-MS, FTIR, and GC from tropical biomass burning, At-mos. Chem. Phys., 7, 5883–5897, doi:10.5194/acp-7-5883-2007, 2007.

Keywood, M., Kanakidou, M., Stohl, A., Dentener, F., Grassi, G., Meyer, C. P., Torseth, K., Edwards, D., Thompson, A., Lohmann, U., and Burrows, J. P.: Fire in the Air–

BB emissions of trace gases and particles in marine air

S. J. Lawson et al.

Title Page

Abstract | Introduction

Conclusions | References

Tables | Figures

◁ | ▷

◁ | ▷

Back | Close

Full Screen / Esc

Printer-friendly Version

Interactive Discussion

Biomass burning impacts in a changing climate, Crit. Rev. Env. Sci. Tec., 43, 40–83, doi:10.1080/10643389.2011.604248, 2011.

Kitchener, A. and Harris, S.: From forest to fjaeldmark: descriptions of Tasmania's vegetation, 2nd Edn., Department of Primary Industries, Parks, Water and Environment, Tasmania, 2013.

Kondo, Y., Matsui, H., Moteki, N., Sahu, L., Takegawa, N., Kajino, M., Zhao, Y., Cubison, M. J., Jimenez, J. L., Vay, S., Diskin, G. S., Anderson, B., Wisthaler, A., Mikoviny, T., Fuelberg, H. E., Blake, D. R., Huey, G., Weinheimer, A. J., Knapp, D. J., and Brune, W. H.: Emissions of black carbon, organic, and inorganic aerosols from biomass burning in North America and Asia in 2008, J. Geophys. Res.-Atmos., 116, D08204, doi:10.1029/2010jd015152, 2011.

Korhonen, H., Carslaw, K. S., Spracklen, D. V., Mann, G. W., and Woodhouse, M. T.: Influence of oceanic dimethyl sulfide emissions on cloud condensation nuclei concentrations and seasonality over the remote Southern Hemisphere oceans: a global model study, J. Geophys. Res.-Atmos., 113, D15204, doi:10.1029/2007jd009718, 2008.

Krummel, P. B., Fraser, P., Steele, L. P., Porter, L. W., Derek, N., Rickard, C., Dunse, B. L., Langenfelds, R. L., Miller, B. R., Baly, S. B., and McEwan, S.: The AGAGE in situ program for non-CO_2 greenhouse gases at Cape Grim, 2005–2006: methane, nitrous oxide, carbon monoxide, hydrogen, CFCs, HCFCs, HFCs, PFCs, halons, chlorocarbons, hydrocarbons and sulphur hexafluoride, in: 2005–2006 Baseline Atmospheric Program (Australia), edited by: Cainey, J. M., Derek, N., and Krummel, P. B., Australian Bureau of Meteorology and CSIRO Marine and Atmospheric Research, Melbourne, 65–77, available at: http://www.bom.gov.au/inside/cgbaps/baseline/Baseline_2005-2006.pdf (last access: 13 May 2015), 2007.

Lawler, M. J., Whitehead, J., O'Dowd, C., Monahan, C., McFiggans, G., and Smith, J. N.: Composition of 15–85 nm particles in marine air, Atmos. Chem. Phys., 14, 11557–11569, doi:10.5194/acp-14-11557-2014, 2014.

Lawson, S. J., Cope, M., Lee, S., Keywood, M., Galbally, I. E., and Ristovski, Z.: Biomass burning at Cape Grim: using modelling to explore plume photochemistry and composition, Atmos. Chem. Phys. Discuss., in preparation, 2015.

Lewis, A. C., Evans, M. J., Hopkins, J. R., Punjabi, S., Read, K. A., Purvis, R. M., Andrews, S. J., Moller, S. J., Carpenter, L. J., Lee, J. D., Rickard, A. R., Palmer, P. I., and Parrington, M.: The influence of biomass burning on the global distribution of selected non-methane organic compounds, Atmos. Chem. Phys., 13, 851–867, doi:10.5194/acp-13-851-2013, 2013.

Title Page

Abstract | Introduction

Conclusions | References

Tables | Figures

|◀ | ▶|

◀ | ▶

Back | Close

Full Screen / Esc

Printer-friendly Version

Interactive Discussion

Lobert, J. M., Keene, W. C., Logan, J. A., and Yevich, R.: Global chlorine emissions from biomass burning: reactive chlorine emissions inventory, J. Geophys. Res.-Atmos., 104, 8373–8389, doi:10.1029/1998jd100077, 1999.

Martin, M., Tritscher, T., Juránvi, Z., Heringa, M. F., Sierau, B., Weingartner, E., Chirico, R., Gysel, M., Prévôt, A. S. H., Baltensperger, U., and Lohmann, U.: Hygroscopic properties of fresh and aged wood burning particles, J. Aerosol Sci., 56, 15–29, doi:10.1016/j.jaerosci.2012.08.006, 2013.

McCulloch, A., Midgley, P. M., and Ashford, P.: Releases of refrigerant gases (CFC-12, HCFC-22 and HFC-134a) to the atmosphere, Atmos. Environ., 37, 889–902, doi:10.1016/S1352-2310(02)00975-5, 2003.

Meyer, C. P. and Cook, G. D.: Biomass combustion and emission processes in the Northern Australian Savannas, in: Carbon Accounting and Savanna Fire Management, edited by: Murphy, B. P., Edwards, A. C., Meyer, C. P., and Russell-Smith, J., CSIRO Publishing, Clayton, Australia, 185–234, 2015.

Meyer, C. P., Cook, G. D., Reisen, F., Smith, T. E. L., Tattaris, M., Russell-Smith, J., Maier, S., Yates, C. P., and Wooster, M. J.: Direct measurements of the seasonality of emission factors from savanna fires in northern Australia, J. Geophys. Res.-Atmos., 117, D20305, doi:10.1029/2012JD017671, 2012.

Miller, B. R., Weiss, R. F., Salameh, P. K., Tanhua, T., Greally, B. R., Mühle, J., and Simmonds, P. G.: Medusa: a sample preconcentration and GC/MS detector system for in situ measurements of atmospheric trace halocarbons, hydrocarbons, and sulfur compounds, Anal. Chem., 80, 1536–1545, doi:10.1021/ac702084k, 2008.

Ortega, A. M., Day, D. A., Cubison, M. J., Brune, W. H., Bon, D., de Gouw, J. A., and Jimenez, J. L.: Secondary organic aerosol formation and primary organic aerosol oxidation from biomass-burning smoke in a flow reactor during FLAME-3, Atmos. Chem. Phys., 13, 11551–11571, doi:10.5194/acp-13-11551-2013, 2013.

Paton-Walsh, C., Jones, N. B., Wilson, S. R., Haverd, V., Meier, A., Griffith, D. W. T., and Rinsland, C. P.: Measurements of trace gas emissions from Australian forest fires and correlations with coincident measurements of aerosol optical depth, J. Geophys. Res.-Atmos., 110, D24305, doi:10.1029/2005jd006202, 2005.

Paton-Walsh, C., Wilson, S. R., Jones, N. B., and Griffith, D. W. T.: Measurement of methanol emissions from Australian wildfires by ground-based solar Fourier transform spectroscopy, Geophys. Res. Lett., 35, L08810, doi:10.1029/2007gl032951, 2008.

Paton-Walsh, C., Deutscher, N. M., Griffith, D. W. T., Forgan, B. W., Wilson, S. R., Jones, N. B., and Edwards, D. P.: Trace gas emissions from savanna fires in northern Australia, J. Geophys. Res.-Atmos., 115, D16314, doi:10.1029/2009jd013309, 2010.

Paton-Walsh, C., Emmons, L. K., and Wiedinmyer, C.: Australia's Black Saturday fires – comparison of techniques for estimating emissions from vegetation fires, Atmos. Environ., 60, 262–270, doi:10.1016/j.atmosenv.2012.06.066, 2012.

Paton-Walsh, C., Smith, T. E. L., Young, E. L., Griffith, D. W. T., and Guérette, É.-A.: New emission factors for Australian vegetation fires measured using open-path Fourier transform infrared spectroscopy – Part 1: Methods and Australian temperate forest fires, Atmos. Chem. Phys., 14, 11313–11333, doi:10.5194/acp-14-11313-2014, 2014.

Petters, M. D., Carrico, C. M., Kreidenweis, S. M., Prenni, A. J., DeMott, P. J., Collett, J. L., and Moosmüller, H.: Cloud condensation nucleation activity of biomass burning aerosol, J. Geophys. Res.-Atmos., 114, D22205, doi:10.1029/2009JD012353, 2009.

Pratt, K. A., Murphy, S. M., Subramanian, R., DeMott, P. J., Kok, G. L., Campos, T., Rogers, D. C., Prenni, A. J., Heymsfield, A. J., Seinfeld, J. H., and Prather, K. A.: Flight-based chemical characterization of biomass burning aerosols within two prescribed burn smoke plumes, Atmos. Chem. Phys., 11, 12549–12565, doi:10.5194/acp-11-12549-2011, 2011.

Prinn, R. G., Weiss, R. F., Fraser, P. J., Simmonds, P. G., Cunnold, D. M., Alyea, F. N., O'Doherty, S., Salameh, P., Miller, B. R., Huang, J., Wang, R. H. J., Hartley, D. E., Harth, C., Steele, L. P., Sturrock, G., Midgley, P. M., and McCulloch, A.: A history of chemically and radiatively important gases in air deduced from ALE/GAGE/AGAGE, J. Geophys. Res.-Atmos., 105, 17751–17792, doi:10.1029/2000JD900141, 2000.

Quinn, P. K. and Bates, T. S.: The case against climate regulation via oceanic phytoplankton sulphur emissions, Nature, 480, 51–56, doi:10.1038/nature10580, 2011.

Sahu, L. K., Kondo, Y., Moteki, N., Takegawa, N., Zhao, Y., Cubison, M. J., Jimenez, J. L., Vay, S., Diskin, G. S., Wisthaler, A., Mikoviny, T., Huey, L. G., Weinheimer, A. J., and Knapp, D. J.: Emission characteristics of black carbon in anthropogenic and biomass burning plumes over California during ARCTAS-CARB 2008, J. Geophys. Res.-Atmos., 117, D16302, doi:10.1029/2011jd017401, 2012.

Shirai, T., Blake, D. R., Meinardi, S., Rowland, F. S., Russell-Smith, J., Edwards, A., Kondo, Y., Koike, M., Kita, K., Machida, T., Takegawa, N., Nishi, N., Kawakami, S., and Ogawa, T.:

Title Page

Abstract | Introduction

Conclusions | References

Tables | Figures

⏮ | ⏭

◀ | ▶

Back | Close

Full Screen / Esc

Printer-friendly Version

Interactive Discussion

Emission estimates of selected volatile organic compounds from tropical savanna burning in northern Australia, J. Geophys. Res.-Atmos., 108, 8406, doi:10.1029/2001jd000841, 2003.

Simpson, I. J., Akagi, S. K., Barletta, B., Blake, N. J., Choi, Y., Diskin, G. S., Fried, A., Fuelberg, H. E., Meinardi, S., Rowland, F. S., Vay, S. A., Weinheimer, A. J., Wennberg, P. O., Wiebring, P., Wisthaler, A., Yang, M., Yokelson, R. J., and Blake, D. R.: Boreal forest fire emissions in fresh Canadian smoke plumes: C_1–C_{10} volatile organic compounds (VOCs), CO_2, CO, NO_2, NO, HCN and CH_3CN, Atmos. Chem. Phys., 11, 6445–6463, doi:10.5194/acp-11-6445-2011, 2011.

Smith, T. E. L., Paton-Walsh, C., Meyer, C. P., Cook, G. D., Maier, S. W., Russell-Smith, J., Wooster, M. J., and Yates, C. P.: New emission factors for Australian vegetation fires measured using open-path Fourier transform infrared spectroscopy – Part 2: Australian tropical savanna fires, Atmos. Chem. Phys., 14, 11335–11352, doi:10.5194/acp-14-11335-2014, 2014.

Steele, L. P., Krummel, P. B., Spencer, D. A., Rickard, C., Baly, S. B., Langenfelds, R. L., and van der Schoot, M. V.: Baseline carbon dioxide monitoring, in: Baseline Atmospheric Program Australia 2005–2006, Australian Bureau of Meteorology and CSIRO Marine and Atmospheric Research, Melbourne, 50–52, available at: http://www.bom.gov.au/inside/cgbaps/baseline.shtml (last access: 13 May 2015), 2007.

Stockwell, C. E., Veres, P. R., Williams, J., and Yokelson, R. J.: Characterization of biomass burning emissions from cooking fires, peat, crop residue, and other fuels with high-resolution proton-transfer-reaction time-of-flight mass spectrometry, Atmos. Chem. Phys., 15, 845–865, doi:10.5194/acp-15-845-2015, 2015.

Vakkari, V., Kerminen, V.-M., Beukes, J. P., Tiitta, P., van Zyl, P. G., Josipovic, M., Venter, A. D., Jaars, K., Worsnop, D. R., Kulmala, M., and Laakso, L.: Rapid changes in biomass burning aerosols by atmospheric oxidation, Geophys. Res. Lett., 41, 2644–2651, doi:10.1002/2014GL059396, 2014.

van Leeuwen, T. T. and van der Werf, G. R.: Spatial and temporal variability in the ratio of trace gases emitted from biomass burning, Atmos. Chem. Phys., 11, 3611–3629, doi:10.5194/acp-11-3611-2011, 2011.

Virkkula, A., Levula, J., Pohja, T., Aalto, P. P., Keronen, P., Schobesberger, S., Clements, C. B., Pirjola, L., Kieloaho, A.-J., Kulmala, L., Aaltonen, H., Patokoski, J., Pumpanen, J., Rinne, J., Ruuskanen, T., Pihlatie, M., Manninen, H. E., Aaltonen, V., Junninen, H., Petäjä, T., Backman, J., Dal Maso, M., Nieminen, T., Olsson, T., Grönholm, T., Aalto, J., Virtanen, T. H.,

Kajos, M., Kerminen, V.-M., Schultz, D. M., Kukkonen, J., Sofiev, M., De Leeuw, G., Bäck, J., Hari, P., and Kulmala, M.: Prescribed burning of logging slash in the boreal forest of Finland: emissions and effects on meteorological quantities and soil properties, Atmos. Chem. Phys., 14, 4473–4502, doi:10.5194/acp-14-4473-2014, 2014.

Volkova, L., Meyer, C. P., Murphy, S., Fairman, T., Reisen, F., and Weston, C.: Fuel reduction burning mitigates wildfire effects on forest carbon and greenhouse gas emission, Int. J. Wildland Fire, 23, 771–780, doi:10.1071/WF14009, 2014.

Vollmer, M. K., Walter, S., Mohn, J., Steinbacher, M., Bond, S. W., Röckmann, T., and Reimann, S.: Molecular hydrogen (H_2) combustion emissions and their isotope (D/H) signatures from domestic heaters, diesel vehicle engines, waste incinerator plants, and biomass burning, Atmos. Chem. Phys., 12, 6275–6289, doi:10.5194/acp-12-6275-2012, 2012.

Watson, J. G., Chow, J. C., Chen, L. W. A., Lowenthal, D. H., Fujita, E. M., Kuhns, H. D., Sodeman, D. A., Campbell, D. E., Moosmüller, H., Zhu, D., and Motallebi, N.: Particulate emission factors for mobile fossil fuel and biomass combustion sources, Sci. Total Environ., 409, 2384–2396, doi:10.1016/j.scitotenv.2011.02.041, 2011.

Wigder, N. L., Jaffe, D. A., and Saketa, F. A.: Ozone and particulate matter enhancements from regional wildfires observed at Mount Bachelor during 2004–2011, Atmos. Environ., 75, 24–31, doi:10.1016/j.atmosenv.2013.04.026, 2013.

Yokelson, R. J., Goode, J. G., Ward, D. E., Susott, R. A., Babbitt, R. E., Wade, D. D., Bertschi, I., Griffith, D. W. T., and Hao, W. M.: Emissions of formaldehyde, acetic acid, methanol, and other trace gases from biomass fires in North Carolina measured by airborne Fourier transform infrared spectroscopy, J. Geophys. Res.-Atmos., 104, 30109–30125, doi:10.1029/1999jd900817, 1999.

Yokelson, R. J., Bertschi, I. T., Christian, T. J., Hobbs, P. V., Ward, D. E., and Hao, W. M.: Trace gas measurements in nascent, aged, and cloud-processed smoke from African savanna fires by airborne Fourier transform infrared spectroscopy (AFTIR), J. Geophys. Res.-Atmos., 108, 8478, doi:10.1029/2002jd002322, 2003.

Yokelson, R. J., Crounse, J. D., DeCarlo, P. F., Karl, T., Urbanski, S., Atlas, E., Campos, T., Shinozuka, Y., Kapustin, V., Clarke, A. D., Weinheimer, A., Knapp, D. J., Montzka, D. D., Holloway, J., Weibring, P., Flocke, F., Zheng, W., Toohey, D., Wennberg, P. O., Wiedinmyer, C., Mauldin, L., Fried, A., Richter, D., Walega, J., Jimenez, J. L., Adachi, K., Buseck, P. R., Hall, S. R., and Shetter, R.: Emissions from biomass burning in the Yucatan, Atmos. Chem. Phys., 9, 5785–5812, doi:10.5194/acp-9-5785-2009, 2009.

Title Page

Abstract | Introduction

Conclusions | References

Tables | Figures

|◀ | ▶|

◀ | ▶

Back | Close

Full Screen / Esc

Printer-friendly Version

Interactive Discussion

Yokelson, R. J., Burling, I. R., Gilman, J. B., Warneke, C., Stockwell, C. E., de Gouw, J., Akagi, S. K., Urbanski, S. P., Veres, P., Roberts, J. M., Kuster, W. C., Reardon, J., Griffith, D. W. T., Johnson, T. J., Hosseini, S., Miller, J. W., Cocker, D. R., Jung, H., and Weise, D. R.: Coupling field and laboratory measurements to estimate the emission factors of identified and unidentified trace gases for prescribed fires, Atmos. Chem. Phys., 13, 89–116, doi:10.5194/acp-13-89-2013, 2013.

Title Page

Abstract   Introduction

Conclusions   References

Tables   Figures

|◄   ►|

◄   ►

Back   Close

Full Screen / Esc

Printer-friendly Version

Interactive Discussion

Table 1. Measurement summary.

Measurement	Instrument	Air intake height	Time resolution	Reference
NMOCs	PTR-MS	10 m	10 min	Galbally et al. (2007a)
Particle size distribution and number 14–700 nm	SMPS	10 m	1 min	Cravigan et al. (2015)
Condensation nuclei (particle number > 3 nm)	TSI particle counters	10 m	1 min	Gras (2007)
black carbon concentration	aethelometer	10 m	integrated 30 min	Gras (2007)
CCN number at 0.5 % SS	CCN counter	10 m	1 min	Gras (2007)
ozone (O_3)	TECO analyser	10 m	1 min	Galbally et al. (2007b)
methane (CH_4)	AGAGE GC-FID	10 m/70 m/75 m	40 min (discrete air sample every 40 min)	Prinn et al. (2000), Krummel et al. (2007)
carbon monoxide (CO) and hydrogen (H_2)	AGAGE GC-MRD	10 m/70 m/75 m	40 min (discrete air sample every 40 min)	Prinn et al. (2000), Krummel et al. (2007)
carbon dioxide (CO_2)	CSIRO LoFlo NDIR	70 m	1 min (continuous analyser)	Steele et al. (2007)
nitrous oxide (N_2O), major CFCs, $CHCl_3$, CH_3CCl_3, CCl_4	AGAGE GC-ECD system	10 m/70 m/75 m	40 min (discrete air sample every 40 min)	Prinn et al. (2000), Krummel et al. (2007)
minor CFCs, HCFCs, HFCs, PFCs, methylhalides, chlorinated solvents, halons, ethane	AGAGE GC-MS-Medusa	75 m	2 h (20 min integrated air sample every 2 h)	Miller et al. (2008), Prinn et al. (2000), Krummel et al. (2007)

Table 2. Summary of periods described in the text for BB1 and BB2 (as shown in Figs. 3 and 6).

Event	Date and Time	Period	Air Mass Origin	Marker Species	Comments
BB1	16 Feb 2006 02:00 AEST	A	Ocean & NW Tasmania	CO, BC, low O_3, particles (uni modal)	Fresh Plume
	16 Feb 2006 06:00 AEST	B	Ocean	O_3, particle growth	Plume processing & dilution
	16 Feb 2006 12:00 AEST	C	mainland Australia	O_3 (overnight enhancement)	Background terrestrial
	17 Feb 2006 06:00 AEST	D	Melbourne	O_3, particles, HFC-134a	Urban
	17 Feb 2006 16:00 AEST	E	Ocean	Particles (bi-modal)	Clean Marine
	18 Feb 2006 00:00 AEST	F	Ocean & mainland Australia	O_3, HFC-134a	Marine with minor terrestrial
BB2	23 Feb 2006 23:00 AEST	A	Ocean & NW Tasmania	CO, BC, Acetonitrile, particles	Fresh Plume
	24 Feb 2006 23:00 AEST	B	mainland Australia	CO, NMOC (Acetonitrile)	Fresh plume + precipitation
	25 Feb 2006 05:00 AEST	C	Melbourne	HFC-134a, O_3	Urban
	25 Feb 2006 23:00 AEST	D	Ocean	Low particles, HFC-134a	Clean Marine

Title Page

Abstract | Introduction

Conclusions | References

Tables | Figures

|◄ | ►|

◄ | ►

Back | Close

Full Screen / Esc

Printer-friendly Version

Interactive Discussion

Table 3. Summary of species measured in BB2 including background concentration, plume concentration, ER to CO and EF.

Compound	formula	Background concentration[a]	BB plume concentration[a]	ER CO[b]	CO ER R^2	EF (g kg^{-1})
Species statistically enhanced in plume		mean (SD)	mean (SD)			
carbon dioxide	CO_2	378.1 (0.7)	382.9 (1.2)	1620	0.15	n/a
carbon monoxide	CO	42 (6)	618 (279)	n/a	n/a	89[c]
methane	CH_4	1713 (2)	1743 (10)	49	0.48	2.5
nitrous oxide	N_2O	319 (0.2)	319.1 (0.2)	0.27	0.01	n/a
hydrogen	H_2	551 (3)	6010 (28)	100	0.87	0.64
ethane	C_2H_6	1845 (146)	1765 (1008)	3.2	0.79	0.30
hydrogen cyanide (m/z 28)	HCN	122 (4)	903 (292)	5.7	0.42	0.49
formaldehyde (m/z 31)	HCHO	541 (339)	1895 (561)	11	0.08	n/a
methanol (m/z 33)	CH_3OH	721 (413)	8603 (2521)	14	0.43	1.4
acetonitrile (m/z 42)	C_2H_3N	35 (4)	983 (324)	1.3	0.58	0.17
acetaldehyde (m/z 45)	CH_3CHO	48 (27)	2608 (807)	4.4	0.53	0.62
unknown (m/z 46)	unknown	105 (72)	279 (74)	0.27	−0.9	n/a
formic acid (m/z 47)	CH_2O_2	19 (7)	141 (63)	0.20	−0.09	n/a
acetone/propanal (m/z 59)	C_3H_6O	170 (31)	1315 (372)	2.0	0.40	0.36
acetic acid (m/z 61)	CH_3COOH	75 (32)	2054 (971)	3.6	0.64	0.52
furan/isoprene (m/z 69)	C_4H_4O	78 (39)	3113 (1139)	5.3	0.72	1.15
MVK/MAK (m/z 71)	C_4H6O	14 (10)	673 (234)	1.2	0.76	0.26
methylglyoxal/methyl ethyl ketone (m/z 73)	C_4H_8O	21 (12)	618 (209)	1.0	0.69	0.24
benzene (m/z 79)	C_6H_6	7 (6)	1093 (390)	1.9	0.78	0.47
unknown (m/z 85)	unknown	15 (5)	847 (276)	1.5	0.51	0.39
unknown (m/z 87)	$C_4H_6O_2$	16 (5)	576 (186)	0.97	0.67	0.27
toluene (m/z 93)	C_7H_8	8 (5)	409 (113)	0.69	0.51	0.20
phenol (m/z 95)	C_6H_5OH	12 (9)	472 (149)	0.80	0.73	0.24
unknown (m/z 101)	Unknown	15 (4)	124 (33)	0.19	0.32	n/a
xylenes (m/z 107)	C_8H_{10}	15 (0)	319 (100)	0.53	0.70	0.18
unknown (m/z 113)	unknown	9 (0)	279 (87)	0.47	0.60	0.17
C_3-benzenes (m/z 121)	C_9H_{12}	20 (12)	290 (89)	0.47	0.73	0.18
monoterpenes (m/z 137)	$C_{10}H_{16}$	17 (9)	219 (79)	0.18	0.51	0.08
unknown (m/z 153)	unknown	45 (135)	91 (29)	0.09	0.61	n/a
methyl chloride	CH_3Cl	5945 (79)	1251 (458)	1.30	0.74	0.21
methyl bromide	CH_3Br	9 (2)	34 (18)	0.05	0.74	0.015
methyl iodide	CH_3I	1.3 (0.2)	3.7 (1.5)	0.004	0.75	0.0019
black carbon	n/a	1.6 (0.3)	1657 (769)	0.003	0.81	0.22
CN > 3 nm	n/a	625 (2078)	24 902 (8031)	38.4	0.7	n/a
CCN 0.5 %	n/a	160 (31)	5501 (1355)	8.3	−0.4	n/a
Species not statistically enhanced in plume						
dimethyl sulphide (m/z 63)	C_2H_6S	158 (57)	172 (15)	n/a	n/a	n/a
chloroform	$CHCl_3$	6.6 (0.5)	8.8 (1.4)	n/a	n/a	n/a
methyl chloroform	CH_3CCl_3	16.1 (0.2)	16.0 (0.2)	n/a	n/a	n/a
dichloromethane	CH_2Cl_2	7.5 (0.04)	7.6 (0.1)	n/a	n/a	n/a
carbon tetrachloride	CCl_4	90.2 (0.7)	90.3 (0.2)	n/a	n/a	n/a
bromoform	$CHBr_3$	4.2 (0.8)	4.7 (0.4)	n/a	n/a	n/a
HFC-32	CH_2F_2	1.02 (0.03)	1.04 (0.03)	n/a	n/a	n/a
HFC-125	C_2HF_5	3.57 (0.04)	3.63 (0.05)	n/a	n/a	n/a
HFC-134a	CH_2FCF_3	33.20 (0.22)	33.28 (0.17)	n/a	n/a	n/a
ozone	O_3	15.1 (1.1)	15.8 (1.5)	n/a	n/a	n/a

[a] Units – all in ppt except for CO, CH_4, N_2O in ppb, CO_2 in ppm, CN and CCN in particles cm^{-3}, BC in ng m^{-3}.

[b] Trace gas emission ratios are molar ratios, BC is mass ratio, particle number is # particles ppb^{-1}.

[c] EF for CO taken from temperate forest (Akagi et al., 2011), n/a = not applicable.

Table 4. Comparison of emission factors with other studies.

	This study $g\,kg^{-1}$ (calculated using Akagi et al., 2011, CO EF of $89\,g\,kg^{-1}$)	Temperate south eastern Australia	Tropical savannah Australia	Temperate Northern Hemisphere
Hydrogen (H_2)	0.64	n/a	n/a	2.03 (1.79)[j]
Methane (CH_4)	2.49	3.5 (1.1)[c]	2.26 (1.27)[d]	3.92 (2.39)[j]
			2.33 (0.80)[e]	3.69 (1.36)[l]
			2.20 (0.32)[f]	
			2.03 (0.13)[h]	
			2.10 (1.16)[i]	
Ethane (C_2H_6)	0.30	0.26 (0.11)[a]	0.60 (0.225)[d]	1.12 (0.67)[j]
		0.5 (0.2)[c]	0.11 (0.09)[e]	0.48 (0.61)[l]
			0.53 (0.02)[f]	
			0.13 (0.04)[g]	
			0.08 (0.05)[i]	
Hydrogen cyanide (HCN)	0.49	0.43 (0.22)[a]	0.036 (0.002)[d]	0.73 (0.19)[j]
			0.025 (0.024)[e]	0.75 (0.26)[l]
			0.11 (0.04)[g]	
			0.53 (0.31)[i]	
Acetonitrile (CH_3CN)	0.17	n/a	0.11 (0.06)[f]	0.15 (0.07)[l]
Acetaldehyde (C_2H_4O)	0.62	n/a	0.55 (0.26)[d]	0.56 (0.40)[l]
			1.0 (0.62)[e]	
Phenol (C_6H_5OH)	0.24	n/a	n/a	0.33 (0.38)[j]
				0.45 (0.19)[l]
Acetic acid (CH_3COOH)	0.52	3.8 (1.3)[c]	1.54 (0.64)[j]	1.97 (1.66)[j]
				1.91 (0.93)[l]
Methanol (CH_3OH)	1.37	2.3 (0.8)[b]	1.06 (0.87)[i]	1.93 (1.38)[j]
		2.4 (1.2)[c]		1.35 (0.4)[l]
Benzene (C_6H_6)	0.47	n/a	0.42 (0.23)[d]	0.45 (0.29)[l]
			0.29 (0.24)[e]	
			0.21 (0.02)[f]	
Toluene (C_7H_8)	0.20	n/a	n/a	0.17 (0.13)[l]
Methyl chloride (CH_3Cl)	0.2082	n/a	0.0605 (0.0072)[f]	0.059[k]
Methyl bromide (CH_3Br)	0.0148	n/a	0.0018 (0.0003)f	0.0036[k]
Methyl iodide (CH_3I)	0.0019	n/a	n/a	0.0008[k]

[a] Paton-Walsh et al. (2005), [b] Paton-Walsh et al. (2008), [c] Paton-Walsh et al. (2014), [d] Hurst et al. (1994a), [e] Hurst et al. (1994b), [f] Shirai et al. (2003), [g] Paton-Walsh et al. (2010), [h] Meyer et al. (2012), [i] Smith et al. (2014), [j] Akagi et al. (2011) temperate, [k] Akagi et al. (2011) extratropical, [l] Yokelson et al. (2013) semi arid shrubland.
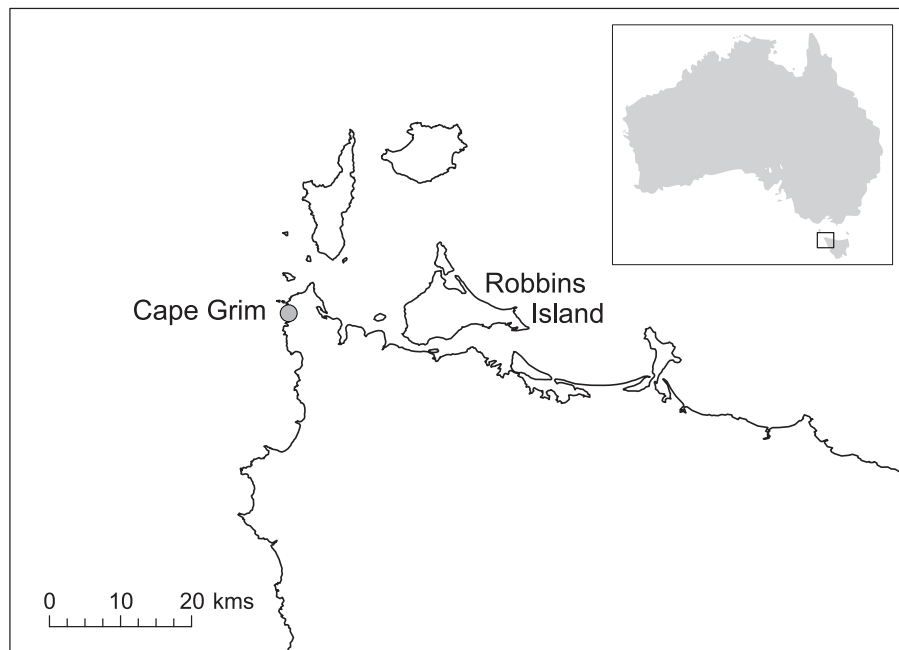
Full Screen / Esc

Figure 1. Location of Cape Grim and Robbins Island in North West Tasmania, Australia.
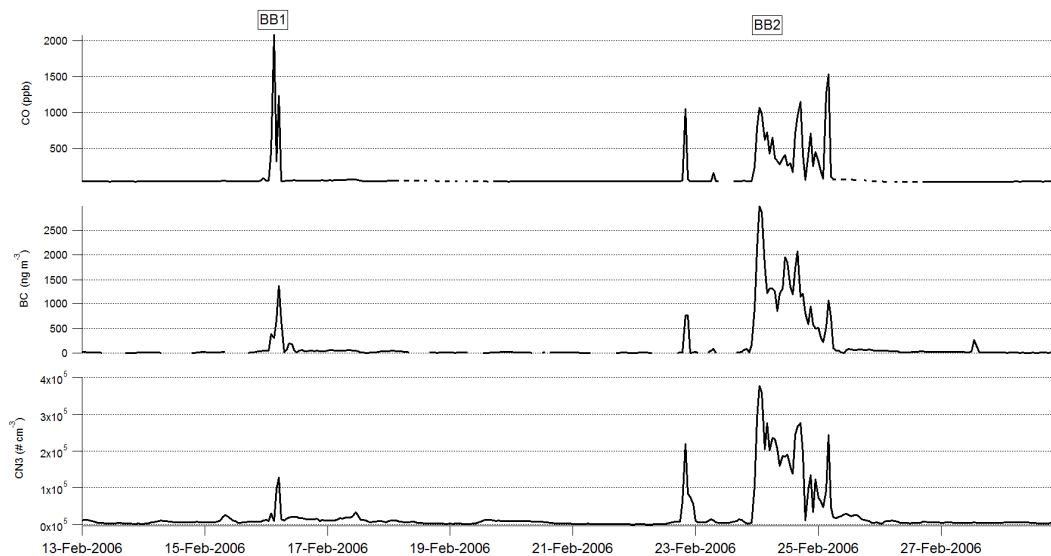
Figure 2. Time series of carbon monoxide (CO), black carbon (BC) and particles > 3 nm (CN3) for the study period (BB1 and BB2 shown).
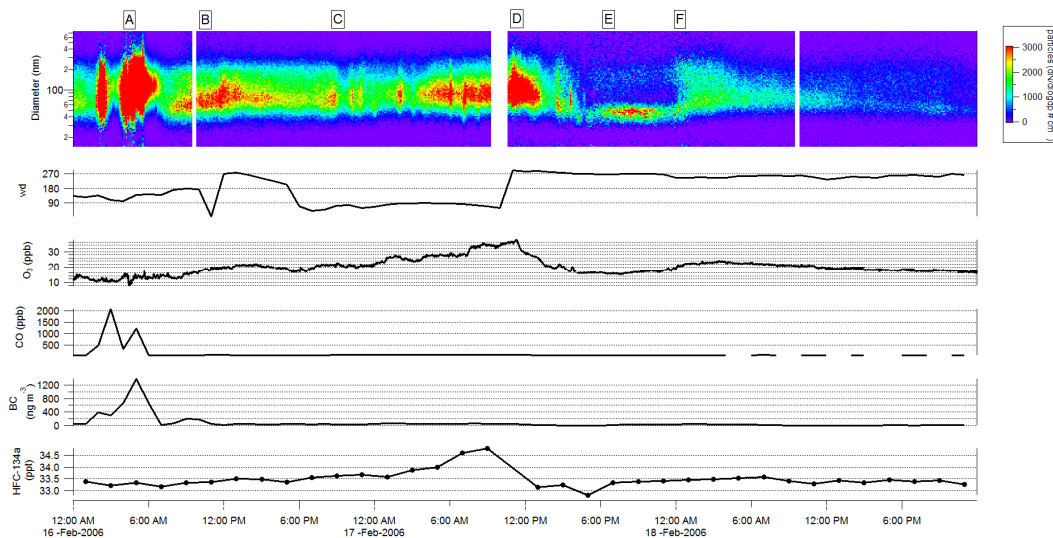
Figure 3. Time series from BB1 including a particle size and number contour plot, wind direction (degrees), ozone (O_3), carbon monoxide (CO), black carbon (BC) and HFC-134a. Periods A–F are discussed in the text.
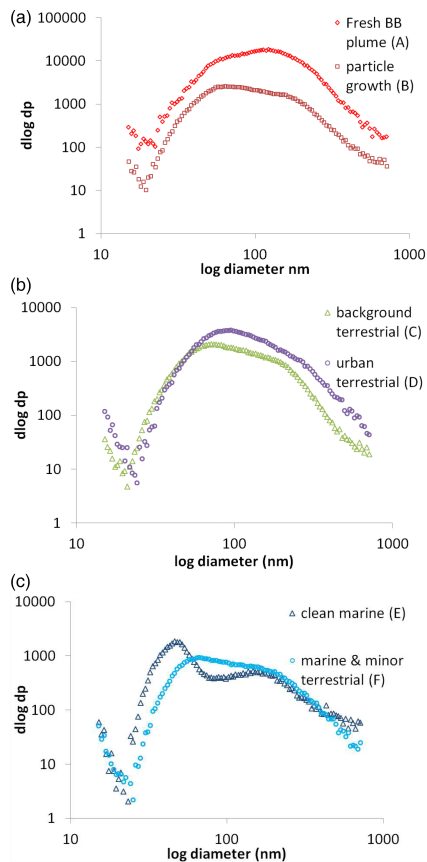
Figure 4. Average particle size distributions (with log scale on both axes) from BB1 corresponding to periods shown in Fig. 3 including **(a)** the fresh plume (period A) and particle growth (period B), **(b)** background terrestrial (period C) and urban terrestrial (period D) and **(c)** clean marine (period E) and marine and minor terrestrial (period F).
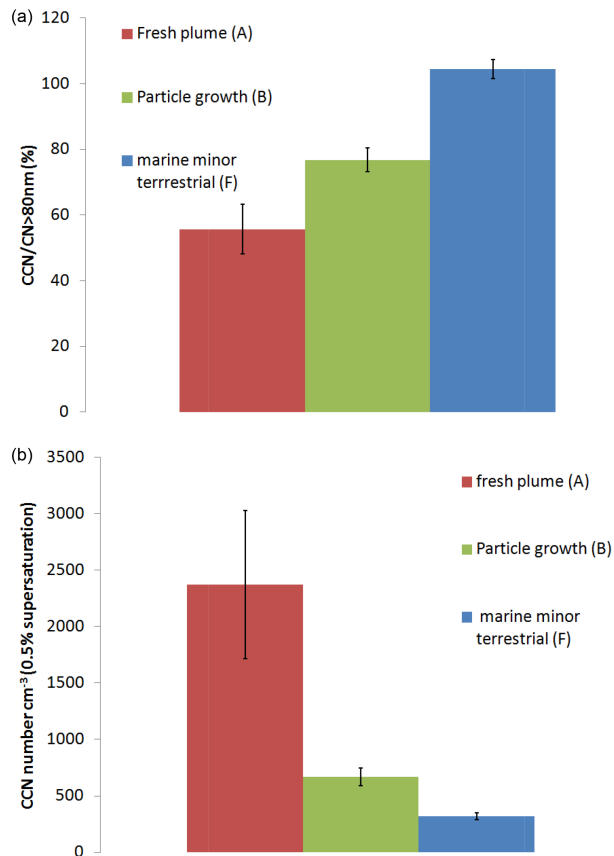
Figure 5. (a) Average ratios of CCN / CN> 80 (hourly) in BB1 during fresh plume (Fig. 3 period A), particle growth event (Fig. 3 period B), and in marine air with minor terrestrial influence (Fig. 3 period F). **(b)** Average absolute number concentrations of CCN (hourly) during the same periods. Error bars are one standard error of the mean.
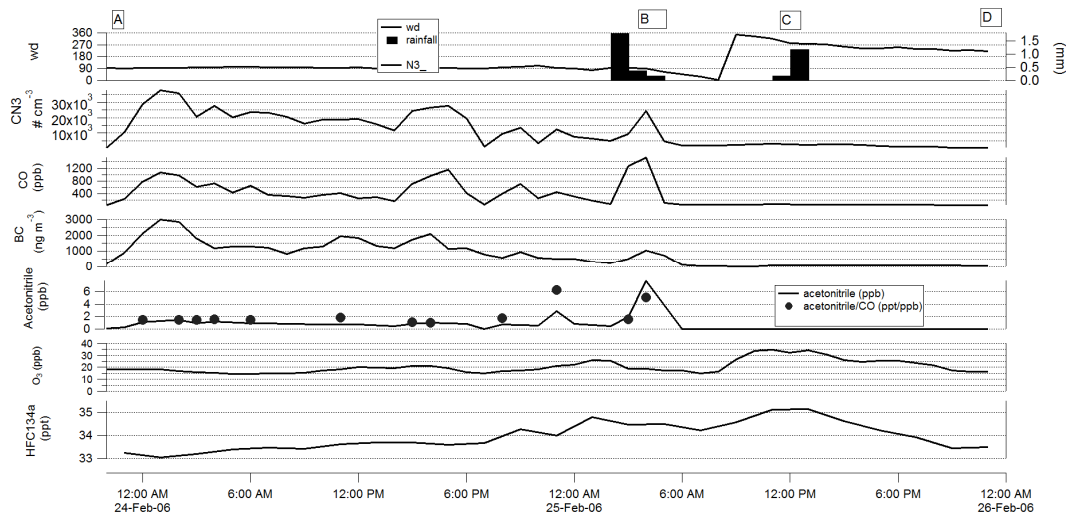
Figure 6. Time series from BB2 including wind direction and rainfall, CN3 (particle number > 3 nm), CO (carbon monoxide), BC (black carbon), acetonitrile and ratio of acetonitrile to CO, O_3 and HFC-134a. Events corresponding to periods A–D are discussed in the text.
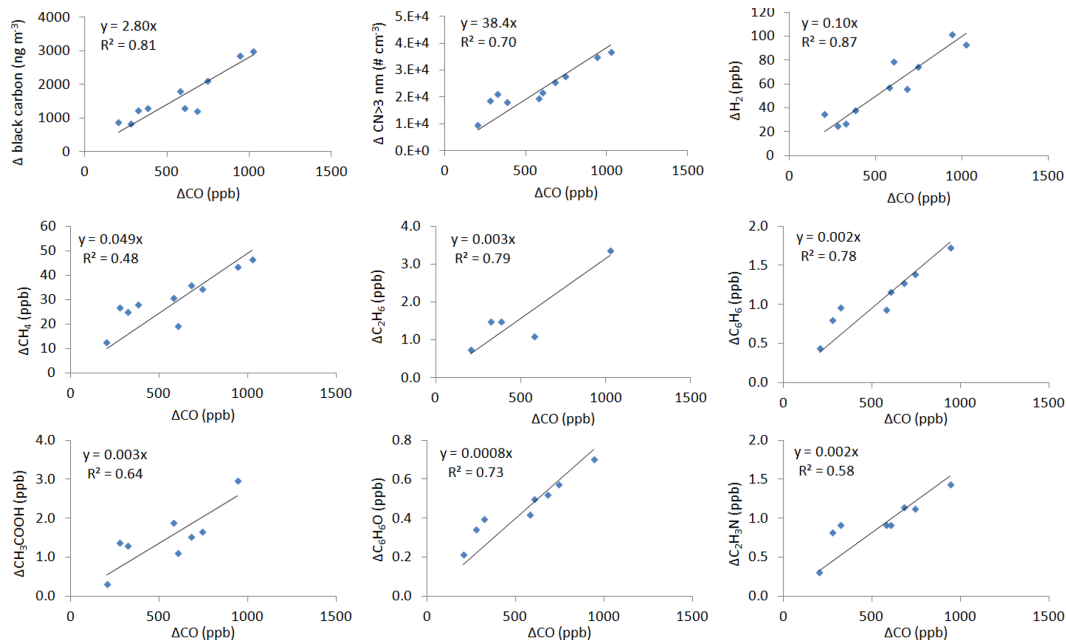
Figure 7. Emission ratios (ER) of several trace gas and aerosol species to CO during period A in BB2.